SYNTHESIS AND CHARACTERIZATION OF POLYPROPYLENE BASED ION-EXCHANGE RESIN

A THESIS SUBMITTED TO
THE GRADUATE SCHOOL OF NATURAL AND APPLIED SCIENCES
OF
MIDDLE EAST TECHNICAL UNIVERSITY

BY

SAFİYE TUBA ECEVİT

IN PARTIAL FULFILLMENT OF THE REQUIREMENTS
FOR
THE DEGREE OF DOCTOR OF PHILOSOPHY
IN
POLYMER SCIENCE AND TECHNOLOGY

MARCH 2012

Approval of the thesis:

SYNTHESIS AND CHARACTERIZATION OF POLYPROPYLENE BASED ION-EXCHANGE RESIN

submitted by **SAFİYE TUBA ECEVİT** in partial fulfillment of the requirements for the degree of **Doctor of Philosophy of Science in Polymer Science and Technology Department, Middle East Technical University** by,

Prof. Dr. Canan Özgen _____
Dean, Graduate School of **Natural and Applied Sciences**

Prof. Dr. Necati Özkan _____
Head of Department, **Polymer Science and Technology**

Prof. Dr. Leyla Aras _____
Supervisor, **Chemistry Department, METU**

Prof. Dr. Teoman Tinçer _____
Co-Supervisor, **Chemistry Department, METU**

Examining Committee Members:

Prof. Dr. Ülkü Yılmazer _____
Chemical Engineering Dept., METU

Prof. Dr. Leyla Aras _____
Chemistry Dept., METU

Prof. Dr. Duygu Kısakürek _____
Chemistry Dept.,METU

Prof. Dr. Göknur Bayram _____
Chemical Engineering Dept., METU

Assoc. Prof. Dr. Cemil Alkan _____
Chemistry Dept., GOU

Date: March 9, 2012

I hereby declare that all information in this document has been obtained and presented in accordance with academic rules and ethical conduct. I also declare that, as required by these rules and conduct, I have fully cited and referenced all materials and rules that are not original to this work.

Name, Last Name : Safiye Tuba ECEVİT

Signature :

ABSTRACT

SYNTHESIS AND CHARACTERIZATION OF POLYPROPYLENE BASED ION EXCHANGE RESIN

Ecevit, Safiye Tuba

Ph.D., Department of Polymer Science and Technology

Supervisor: Prof. Dr. Leyla Aras

Co-Supervisor: Prof. Dr. Teoman Tinçer

March 2012, 97 pages

The synthesis of ion-exchange resin which can be used in various separation and chemical purposes, such as diffusion dialysis, electro dialysis, electrolysis and fuel cells has of considerable interest. For all these applications, the interactions of the ionic groups and the resulted morphologies are critical for establishing the unique properties. Considerable researches have been continued to understand the microstructure of these materials. The aim of this study is to synthesize polypropylene (PP) based ion exchange resins and to investigate their ion-exchange properties.

In the first part of this study polypropylene was functionalized by grafting maleic anhydride onto the polypropylene and the product was characterized by ATR. The effect of maleic anhydride introduced to the grafting medium and the effect of the radical initiator on the maleic anhydride content of the MA-g-PP samples were investigated.

In the second part, neutralization of the MA-g-PP samples with Na^{+}, K^{+}, Mg^{2+} and Ca^{2+} ions and peroxide cross-linking of neutralized MA-g-PP samples were performed. Characterization of the neutralized MA-g-PP samples were performed by ATR and SEM-EDX.

In the last part of the study, ion exchange properties of MA-g-PP resins towards Cu^{2+}, Co^{2+}, Cd^{2+}, Pb^{2+} and Fe^{3+} ions at different pHs were investigated by batch equilibrium method. Rate of metal uptake, concentration effect on the metal uptake and regeneration of the MA-g-PP samples were also examined.

Keywords: Polypropylene, ion exchange resin**,** maleic anhydride-g-polypropylene.

ÖZ

POLİPROPİLEN BAZLI İYON DEĞİŞTİRİCİ REÇİNE SENTEZİ VE KARAKTERİZASYONU

Ecevit, Safiye Tuba
Doktora, Polimer Bilim ve Teknolojisi Bölümü
Tez Yöneticisi: Prof. Dr. Leyla Aras
Ortak Tez Yöneticisi: Prof. Dr. Teoman Tinçer

Mart 2012, 97 sayfa

Difüzyon diyalizi, elektro diyaliz, elektroliz ve yakıt hücreleri gibi çeşitli ayırma ve kimyasal amaçlarda kullanılabilen iyon değişimli reçinelerinin sentezlenmesi kayda değer bir ilgiye sahiptir. Bütün bu uygulamalar için iyonik grupların etkileşimleri ve sonuçlanan morfolojiler benzersiz özelliklerin yapılandırılmasında önemlidir. Bu malzemelerin mikro yapılarının anlaşılması için birçok kayda değer araştırma yapılmış ve devam etmektedir. Bu çalışmanın amacı iyonik fonksiyonel gruplara sahip polipropilen (PP) bazlı reçineler sentezlemek ve bunların iyon değişimi özelliklerinin araştırılmasıdır.

Bu çalışmanın ilk kısmında maleik anhidritin (MA) polipropilene aşı polimerizasyonu gerçekleştirilerek polipropilenin fonksiyonelleştirilmesi sağlandı ve elde edilen örnekler için ATR ile karakterize edildi. Aşı polimerizasyonu sırasında ortama eklenen maleik anhidrit ve radikal miktarının sentezlenen MA-g-PP örneklerindeki maleik anhidrit derecesine olan etkisi gösterildi.

İkinci kısımda, MA-g-PP örnekleri Na^{+}, K^{+}, Mg^{2+} ve Ca^{2+} iyonları ile nötralize edilmiş ve nötralize edilen bu örneklerin peroksit kullanarak çapraz bağlanmaları gerçekleştirilmiştir. Sentezlenen reçinler ATR ve SEM-EDX ile karakterize edilmiştir.

Çalışmanın son kısmında ise sentezlenen reçinelerin iyon değiştirici özellikleri Co^{2+}, Cd^{2+}, Pb^{2+} ve Fe^{3+} iyonları için farklı pH ortamlarda araştırılmıştır. MA-g-PP örneklerinin metal tutma hızları, derişimin metal tutmadaki etkisi ve örneklerin rejenerasyonu da ayrıca araştırılmıştır.

Anahtar Kelimeler: Polipropilen, iyon değiştirici reçine**,** maleik anhidrit-g-polipropilen.

To My Parents

For their love and patience

ACKNOWLEDGEMENTS

I express my gratitude to my supervisor, Prof. Dr. Leyla Aras, for her valuable guidance, support, patience and continual encouragement throughout the success of this work.

I would like to give great thanks to my co-supervisor, Prof. Dr. Teoman Tinçer for his support, guidance, helps and his time and deliberative consideration of this work.

I give many thanks to Prof. Dr. Duygu Kısakürek, Prof. Dr. Göknur Bayram and Assoc. Prof. Dr. Cemil Alkan for their support, encouragement and for spending their time and interesting in my PhD.

Special thanks to Prof. Dr. Yavuz Ataman for his support, guidance and help and to Yasin Arslan and Gamze Karaman for their help during the atomic absorption spectroscopy measurements. For being a hospitable laboratory, many thanks go to the members of D-49, B-36 and B-39 research groups.

I also wish to express my thanks to my friends Arzu Yavuz, Yasin Kanbur, Dilek Okuş, Selahattin Erdoğan and Emsal Uğur for their endless help, moral support and big-hearted friendship during my study.

I would like to extend special thanks to Osman Yaslıtaş for his technical supports.

Last, but not least, I thank my mother, father and brothers for their patience, support and constant encouragement. Appreciation is extended to colleagues in the Department of Chemistry, METU.

TABLE OF CONTENTS

ABSTRACT……..…….……..iv
ÖZ……..…….……..…vi
ACKNOWLEDGEMENTS……..…….……...ix
TABLE OF CONTENTS……..x
LIST OF FIGURES……xiv
LIST OF TABLES……xvii
ABBREVIATIONS……...xxii

CHAPTERS
1. INTRODUCTION
1.1 Ion Exchange…….……..…..……..1
1.2. Ion Exchangers……..…..……..3
1.2.1 Ion Exchange Resins……...……4
1.2.2 General Properties of Ion Exchange Resins……...5
1.2.2.1 Functionality ……..5
1.2.2.2 Capacity……..8
1.2.2.3 Selectivity……...8
1.2.2.4 Crosslinking ……...9
1.2.2.5 Physical Structure of Ion Exchange Resins……9
1.2.3 Application of Ion Exchangers……12
1.3 Polypropylene…….……..13
1.4 Modification of Polypropylene…….……16
1.5 Melt Grafting of Maleic Anhydride on to Polypropylene ……...17
1.6 Peroxide Crosslinking of Polypropylene……..20
1.7 Aim of the Study……...21

2. EXPERIMENTAL……...22
2.1 Materials……...22
2.2 Instrumentation and Method…….22
2.2.1 Mixing……...22
2.2.2 Melt Flow Index (MFI)…….24
2.2.3 Attenuated Total Internal Reflection (ATR) Infrared Micro Spectroscopic Imaging System……..25
2.2.4 Scanning Electron Microscopy (SEM)…….25
2.2.5 Scanning Electron Microscopy-Energy Dispesive X-ray Spectroscopy……..25
2.3 Ion exchange characterization …….26
2.3.1 Batch Equilibrium method……....26
2.3.2 Atomic Absorption Spectoctroscopy……...….26
2.4 Experimental Procedure……26
2.4.1 Melt Grafting of Maleic Anhydride onto Polypropylene…….26
2.4.2 Purification……...27
2.4.3 Determination of the Maleic Anhydride Content of the MA-g-PP by Volumetric Titration……..28
2.4.4 Melt Flow Index……...29
2.4.5 Neutralization of the MA-g-PP with Metal Salts…….29
2.4.6 Characterization of Neutralized MA-g-PP Samples by ATR ……..30
2.4.7 Crosslinking of Neutralized MA-g-PP samples……...30
2.4.8 Characterization of Crosslinked Resins……30
2.4.8.1 Swelling Index Determination……..30
2.4.8.2 Gel Content Determination……...31
2.4.9 Morphological Analysis……32
2.4.9.1 SEM……..32
2.4.9.2 SEM-EDX…….32
2.4.10 Characterization of Ion Exchange Properties ……...…….32

2.4.10.1 Determination of the Ion Exchange Capacity of MA-g-PP……...32
2.4.10.2 Evaluation of Metal Uptake at Different pHs……....33
2.4.10.3 Evaluation of the Concentration Effect on Metal Uptake..35
2.4.10.4 Evaluation of Rate of Metal Uptake……...…35
2.4.10.5 Regeneration Evaluation ……35
3. RESULTS AND DISCUSSION……..36
3.1 Determination of the Maleic Anhydride Content of the MA-g-PP by Volumetric Titration……...36
3.2 Melt Flow Index ……..38
3.3 IR Spectroscopy……39
3.4 Characterization of Crosslinked Resins……45
3.4.1 Swelling Index……..45
3.4.2 Gel Content……...46
3.5 Morphological Analysis Morphology……...47
3.5.1 SEM……..47
3.5.1 SEM-EDX……51
3.6 Characterization of Ion Exchange Properties……...53
3.6.1 Ion Exchange Capacity…….53
3.6.2 Metal Uptake at Different pHs…….53
3.6.2.1 Pb^{2+} Uptake of Ca^{2+} Neutralized MA-g-PP Resin……...……..55
3.6.2.2 Cd^{2+} Uptake of Ca^{2+} Neutralized MA-g-PP Resin……...……..57
3.6.2.2 General Evaluation of Fe^{3+} Uptake……...……...……..59
3.6.3 Evaluation of Concentration Effect on Metal Uptake……...…..…62
3.6.4 Evaluation of Rate of Metal Uptake…….64
3.6.5 Regeneration…….65
4. CONCLUSION……66

REFERENCES……69
APPENDICES……74
A. UPTAKE TEST RESULTS OF Ca^{2+} NEUTRALIZED MA-g-PP RESIN……74
B. UPTAKE TEST RESULTS OF Na^{+} NEUTRALIZED MA-g-PP RESIN…...…….77
C. UPTAKE TEST RESULTS OF Mg^{2+} NEUTRALIZED MA-g-PP RESIN……....82
D. UPTAKE TEST RESULTS OF K^{+} NEUTRALIZED MA-g-PP RESIN……...……87
E. UPTAKE TEST RESULTS OF NON-NEUTRALIZED MA-g-PP RESIN……...…….92
CURRICULUM VITA……97

LIST OF FIGURES

FIGURES

Figure 1.1 Equivalent character of ion exchange……...…..2

Figure 1.2 Schematic representations of polymeric ion exchangers……....4

Figure1.3 The structure of sulphonated polystyrene crosslinked with divinyl benzene……..…6

Figure 1.4 The structure of copolymers of phenol with formaldehyde……....7

Figure 1.5 Copolymer of polyacrylic or polymethacrylic acid with divinylbenzene...7

Figure 1.6 Morphology of ion exchangers……..……....10

Figure 1.7 Distribution of polymeric chains in ion exchangers…….....11

Figure 1.8 Illustration of the macroreticular resin and micrograph of macroporous resin…….....11

Figure 1.9 Propylene monomer……...…13

Figure 1.10 Structures of isotactic, syndiotactic and atactic polypropylenes..……...13

Figure 1.11 The 3^1 helical conformation of isotactic PP in crystalline state…….….14

Figure 1.12 The possible reaction mechanism for the grafting of MA onto the PP...18

Figure 1.13 Main reactional path for the grafting of PP with MA…….……19

Figure 1.14 Scission and crosslinking of polypropylene……20

Figure 2.1 Brabender Plasti-Coder Torque Rheometer model PLV 151 ……..23

Figure 2.2 Schematic diagram of an internal roller mixer …….23

Figure 2.3 Melt Flow Index Instrument…….…….24

Figure 2.4 Neutralization reaction of MA-g-PP with metal salts……...…29

Figure 3.1 Grafting degree of MA-g-PP as a function of loading concentration of MA……...37

Figure 3.2 MFI values of MA-g-PPas afunction of loading concentration of MA.....39

Figure 3.3 ATR spectrum of purified PP sample……40

Figure 3.4 ATR spectrum of MA-g-PP sample collected from brabender ……40

Figure 3.5 ATR spectrum of MA-g-PP purified samples ……..……...41
Figure 3.6 ATR spectrum of MA-g-PP samples subjected to the heat treatment after purification…….…..41
Figure 3.7 The suggested structures of the MA-g-PP samples and assignment of their characteristic IR absorption bands……...……42
Figure 3.8 ATR spectrum of the MA-g-PP sample neutralized with Na^+ ion…...….43
Figure 3.9 ATR spectrum of the MA-g-PP sample neutralized with Mg^{2+} ion…….44
Figure 3.10 ATR spectrum of the MA-g-PP samples neutralized with Ca^{2+} ion…...44
Figure 3.11 ATR spectrums of the MA-g-PP samples neutralized with K^+ ion ...…45
Figure 3.12 The SEM micrograph of purified PP……...47
Figure 3.13 The SEM micrograph of purified MA-g-PP resin……...…48
Figure 3.14 The SEM micrograph of Na^+ neutralized MA-g-PP resin……...……49
Figure 3.15 The SEM micrograph of Ca^{2+} neutralized MA-g-PP resin.……...…49
Figure 3.16 The SEM micrograph of Mg^{2+} neutralized MA-g-PP resin. ……..…50
Figure 3.17 The SEM micrograph of K^+ neutralized MA-g-PP resin……...….50
Figure 3.18 SEM-EDX Element analysis of Na^{2+} neutralized MA-g-PP resin ….…51
Figure 3.19 SEM-EDX Element analysis of Ca^{2+} neutralized MA-g-PP resin…..….51
Figure 3.20 SEM-EDX Element analysis of Mg^{2+} neutralized MA-g-PP resin…….52
Figure 3.21 SEM-EDX Element analysis of K^{2+} neutralized MA-g-PP resin ...……52
Figure 3.22 Calibration curve for Pb^{2+} ion in Pb^{2+} uptake testing of Ca^{2+} neutralized MA-g-PP resin. .……..…55
Figure 3.23 Calibration curve for Cd^{2+} ion in Cd^{2+} uptake testing of Ca^{2+} neutralized MA-g-PP resin. .……..…58
Figure 3.24 Calibration curve for Fe^{3+} ion…….….60
Figure 3.25 Calibration curve for Pb^{2+} ion in concentration effect test ……..……...63
Figure A.1 Calibration curve for Co^{2+} ion in Co^{2+} uptake testing of Ca^{2+} neutralized MA-g-PP resin…….74
Figure A.2 Calibration curve for Cu^{2+} ion in Cu^{2+} uptake testing of Ca^{2+} neutralized MA-g-PP resin…….75

Figure B.1 Calibration curve for Co^{2+} ion in Co^{2+} uptake testing of Na^{+} neutralized MA-g-PP resin……77
Figure B.2 Calibration curve for Pb^{2+} ion in Pb^{2+} uptake testing of Na^{+} neutralized MA-g-PP resin……78
Figure B.3 Calibration curve for Cu^{2+} ion in Cu^{2+} uptake testing of Na^{+} neutralized MA-g-PP resin. ……..79
Figure B.4 Calibration curve for Cd^{2+} ion in Cd^{2+} uptake testing of Na^{+} neutralized MA-g-PP resin. ……...81
Figure C.1 Calibration curve for Co^{2+} ion in Co^{2+} uptake testing of Mg^{2+} neutralized MA-g-PP resin.……...……82
Figure C.2 Calibration curve for Pb^{2+} ion in Pb^{2+} uptake testing of Mg^{2+} neutralized MA-g-PP resin..……..…83
Figure C.3 Calibration curve for Cu^{2+} ion in Cu^{2+} uptake testing of Mg^{2+} neutralized MA-g-PP resin……84
Figure C.4 Calibration curve for Cd^{2+} ion in Cd^{2+} uptake testing of Mg^{2+} neutralized MA-g-PP resin……86
Figure D.1 Calibration curve for Co^{2+} ion in Co^{2+} uptake testing of K^{+} neutralized MA-g-PP resin……87
Figure D.2 Calibration curve for Pb^{2+} ion in Pb^{2+} uptake testing of K^{+} neutralized MA-g-PP resin..……...…89
Figure D.3 Calibration curve for Cu^{2+} ion in Cu^{2+} uptake testing of K^{+} neutralized MA-g-PP resin...……..……90
Figure D.4 Calibration curve for Cd^{2+} ion in Cd^{2+} uptake testing of K^{+} neutralized MA-g-PP resin……..…91
Figure E.1 Calibration curve for Co^{2+} ion in Co^{2+} uptake testing for non-neutralized MA-g-PP resin..……92
Figure E.2 Calibration curve for Pb^{2+} ion in Pb^{2+} uptake testing for non-neutralized MA-g-PP resin…….94

Figure E.3 Calibration curve for Cu^{2+} ion in Cu^{2+} uptake testing for non-neutralized MA-g-PP resin..……...95
Figure E.4 Calibration curve for Cd^{2+} ion in Cd^{2+} uptake testing for non-neutralized MA-g-PP resin……...…….96

LIST OF TABLES

TABLES

Table 1.1 Functional groups of ion exchange resins……6

Table 2.1 The reaction compositions of grafted samples……27

Table 2.2 Composition of acetate buffer solutions……..……...…34

Table 3.1 Maleic anhydride content of MA-g-PP samples…….36

Table 3.2 MFI of MA-g-PP samples prepared……38

Table 3.3 Swelling indexes of the resins…….……45

Table 3.4 The cross-linking degree of the resins……46

Table 3.5 Summary of the metal uptake results of MA-g-PP resins……...54

Table 3.6 Absorbance values for Pb^{2+} ion standard solutions in Pb^{2+} uptake testing of Ca^{2+} neutralized MA-g-PP resin. ……..…..55

Table 3.7 Absorbance values for Pb^{2+} of the filtrate solutions in Pb^{2+} uptake testing of Ca^{2+} neutralized MA-g-PP resin……...……...…56

Table 3.8 Pb^{2+} ion concentrations uptaken by Ca^{2+} neutralized MA-g-PP resin and Pb^{2+} uptake values for Ca^{2+} neutralized MA-g-PP resin. …….……..…57

Table 3.9 Absorbance values for Cd^{2+} ion standard solutions in Cd^{2+} uptake testing of Ca^{2+} neutralized MA-g-PP resin……....57

Table 3.10 Absorbance values for Cd^{2+} of the filtrate solutions in Cd^{2+} uptake testing of Ca^{2+} neutralized MA-g-PP resin.…… ……..……..58

Table 3.11 Cd^{2+} ion concentrations of the filtrate solutions and Cd^{2+} uptake values for Ca^{2+} neutralized MA-g-PP resin.…… ……59

Table 3.12 Absorbance values for Fe^{3+} ion standard solutions……...60

Table 3.13 Absorbance values for Fe^{3+} of the filtrate solutions in Fe^{3+} uptake testing of Ca^{2+}, Mg^{2+}, Na^{+}, K^{+} neutralized and non-neutralized MA-g-PP resins ……....61

Table 3.14 Fe^{3+} ion concentrations uptaken by resins and Fe^{3+} uptake values for resins……..…..62

Table 3.15 Absorbance values for Pb^{2+} ion standard solutions……..….62
Table 3.16 Absorbance values for Pb^{2+} of the filtrate solutions in concentration effect test..……..63
Table 3.17 Pb^{2+} uptake values for for Ca^{2+} neutralized MA-g-PP resins ……...…63
Table 3.18 Rates of metal ion uptake of Ca^{2+} neutralized MA-g-PP resin……..…..64
Table 3.19 The percent regeneration of the resins……..65
Table A.1 Absorbance values for Co^{2+} ion standard solutions in Co^{2+} uptake testing of Ca^{2+} neutralized MA-g-PP resin……..…74
Table A.2 Absorbance values for Co^{2+} of the filtrate solutions in Co^{2+} uptake testing of Ca^{2+} neutralized MA-g-PP resin after the incubation period.……75
Table A.3 Absorbance values for Cu^{2+} ion standard solutions in Cu^{2+} uptake testing of Ca^{2+} neutralized MA-g-PP resin.……75
Table A.4 Absorbance values for Cu^{2+} of the filtrate solutions in Cu^{2+} uptake testing of Ca^{2+} neutralized MA-g-PP resin after the incubation period……..……76
Table B.1 Absorbance values for Co^{2+} ion standard solutions in Co^{2+} uptake testing of Na^{+} neutralized MA-g-PP resin.……77
Table B.2 Absorbance values for Co^{2+} of the filtrate solutions in Co^{2+} uptake testing of Na^{+} neutralized MA-g-PP resin after the incubation period……..……..…78
Table B.3 Absorbance values for Pb^{2+} ion standard solutions in Pb^{2+} uptake testing of Na^{+} neutralized MA-g-PP resin……..…78
Table B.4 Absorbance values for Pb^{2+} of the filtrate solutions in Pb^{2+} uptake testing of Na^{+} neutralized MA-g-PP resin after the incubation period……...…79
Table B.5 Absorbance values for Cu^{2+} ion standard solutions in Cu^{2+} uptake testing of Na^{+} neutralized MA-g-PP resin……...79
Table B.6 Absorbance values for Cu^{2+} of the filtrate solutions in Cu^{2+} uptake testing of Na^{+} neutralized MA-g-PP resin after the incubation period……...80
Table B.7 Absorbance values for Cd^{2+} ion standard solutions in Cd^{2+} uptake testing of Na^{+} neutralized MA-g-PP resin……..…80

Table B.8 Absorbance values for Cd^{2+} of the filtrate solutions in Cd^{2+} uptake testing of Na^{+} neutralized MA-g-PP resin after the incubation period……...…81
Table C.1 Absorbance values for Co^{2+} ion standard solutions in Co^{2+} uptake testing of Mg^{2+} neutralized MA-g-PP resin…….82
Table C.2 Absorbance values for Co^{2+} of the filtrate solutions in Co^{2+} uptake testing of Mg^{2+} neutralized MA-g-PP resin after the incubation period……..83
Table C.3 Absorbance values for Pb^{2+} ion standard solutions in Pb^{2+} uptake testing of Mg^{2+} neutralized MA-g-PP resin…….83
Table C.4 Absorbance values for Pb^{2+} of the filtrate solutions in Pb^{2+} uptake testing of Mg^{2+} neutralized MA-g-PP resin after the incubation period……..84
Table C.5 Absorbance values for Cu^{2+} ion standard solutions in Cu^{2+} uptake testing of Mg^{2+} neutralized MA-g-PP resin…….84
Table C.6 Absorbance values for Cu^{2+} of the filtrate solutions in Cu^{2+} uptake testing of Mg^{2+} neutralized MA-g-PP resin after the incubation period……..…85
Table C.7 Absorbance values for Cd^{2+} ion standard solutions in Cd^{2+} uptake testing of Mg^{2+} neutralized MA-g-PP resin…….....85
Table C.8 Absorbance values for Cd^{2+} of the filtrate solutions in Cd^{2+} uptake testing of Mg^{2+} neutralized MA-g-PP resin after the incubation period…….86
Table D.1 Absorbance values for Co^{2+} ion standard solutions in Co^{2+} uptake testing of K^{+} neutralized MA-g-PP resin……87
Table D.2 Absorbance values for Co^{2+} of the filtrate solutions in Co^{2+} uptake testing of K^{+} neutralized MA-g-PP resin after the incubation period…….88
Table D.3 Absorbance values for Pb^{2+} ion standard solutions in Pb^{2+} uptake testing of K^{+} neutralized MA-g-PP resin…….88
Table D.4 Absorbance values for Pb^{2+} of the filtrate solutions in Pb^{2+} uptake testing of K^{+} neutralized MA-g-PP resin after the incubation period……....89
Table D.5 Absorbance values for Cu^{2+} ion standard solutions in Cu^{2+} uptake testing of K^{+} neutralized MA-g-PP resin……89

Table D.6 Absorbance values for Cu^{2+} of the filtrate solutions in Cu^{2+} uptake testing of K^+ neutralized MA-g-PP resin after the incubation period……90
Table D.7 Absorbance values for Cd^{2+} ion standard solutions in Cd^{2+} uptake testing of K^+ neutralized MA-g-PP resin……90
Table D.8 Absorbance values for Cd^{2+} of the filtrate solutions in Cd^{2+} uptake testing of K^+ neutralized MA-g-PP resin after the incubation period……91
Table E.1 Absorbance values for Co^{2+} ion standard solutions in Co^{2+} uptake testing of non-neutralized MA-g-PP resin……..92
Table E.2 Absorbance values for Co^{2+} of the filtrate solutions in Co^{2+} uptake testing of non-neutralized MA-g-PP resin after the incubation period……...93
Table E.3 Absorbance values for Pb^{2+} ion standard solutions in Pb^{2+} uptake testing of non-neutralized MA-g-PP resin……...93
Table E.4 Absorbance values for Pb^{2+} of the filtrate solutions in Pb^{2+} uptake testing of non-neutralized MA-g-PP resin after the incubation period……...94
Table E.5 Absorbance values for Cu^{2+} ion standard solutions in Cu^{2+} uptake testing of non-neutralized MA-g-PP resin……...94
Table E.6 Absorbance values for Cu^{2+} of the filtrate solutions in Cu^{2+} uptake testing of non-neutralized MA-g-PP resin after the incubation period……..…….95
Table E.7 Absorbance values for Cd^{2+} ion standard solutions in Cd^{2+} uptake testing of non-neutralized MA-g-PP resin……..95
Table E.8 Absorbance values for Cd^{2+} of the filtrate solutions in Cd^{2+} uptake testing of non- neutralized MA-g-PP resin after the incubation period……...96

ABBREVIATIONS

AAS	Atomic absorption spectroscopy
ATR	Attenuated total internal reflection
$Ca(C_{17}H_{35}COO)_2$	Calcium stearate
DCP	Dicumyl peroxide
EDX	Energy dispersive X-ray spectroscopy
KOH	Potassium hydroxide
MA	Maleic anhydride
MA-g-PP	Maleic anhydride grafted polypropylene
MFI	Melt flow index
$Mg(C_2H_3O_2)_2.4(H_2O)$	Magnesium acetate
NaOH	Sodium hydroxide
PP	Polypropylene
SEM	Scanning electron microscopy

CHAPTER 1

INTRODUCTION

1.1. Ion Exchange

Ion exchange can be defined as the reversible interchange of ions between a solid phase (the ion exchanger) and a solution phase. It resembles sorption in that, in both cases a dissolved species is taken up by a solid. The characteristic difference between the two phenomena is that ion exchange, in contrast to sorption, is a stoichiometric process. Every ion which is removed from the solution is replaced by an equivalent amount of another ionic species of the same sign. In sorption, on the other hand, a solute (an electrolyte or non-electrolyte) is taken up without being replaced by another species [1, 2]. The stoichiometric character of the process is illustrated in Figure 1.1.

Although this distinction seems clear-cut, it is difficult to apply in practice, since ion-exchange process is accompanied by electrolyte sorption or desorption. In addition to this, ion exchange process takes place both on the pore surface or in the bulk of the material, so using the term *sorption* is more suitable than *adsorption*. Thus; *a*lthough the term *sorption* itself does not suggest a necessity of the stoichiometry, ion exchange itself can be considered as a kind of sorption interaction [2].

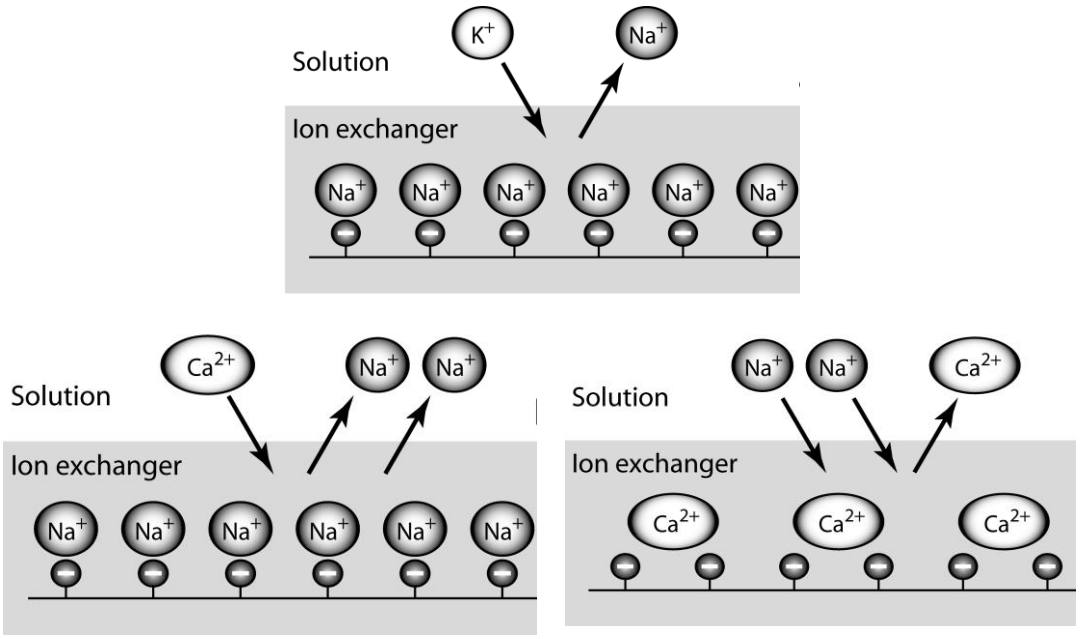

Figure 1.1. Equivalent character of ion exchange [2].

If an ion exchanger R^-A^+, carrying cations A^+ as the exchanger ions, is placed in an aqueous solution phase containing B^+ cations and the ion exchanger has a greater affinity for ion B^+ than for ion A^+, an ion exchange reaction takes place which may be represented by the following equation where R represents the ion exchanger:

$$R^-A^+ + B^+ \leftrightarrows R^-B^+ + A^+ \quad (1)$$

A mass action relationship applies where the bracketed entities represent concentrations:

$$\frac{[BR][A]}{[AR][B]} = Q \quad (2)$$

Q is the equilibrium quotient, and is a constant specific for the pair of ions and type of resin. This expression indicates that if a concentrated solution containing ion A is

now passed through the exhausted bed, the resin will regenerate into the AR form ready for re-use, whilst ion B will be eluted into water. All large scale applications for ion exchange resins involve such exhaustion and regeneration cycles [3].

1.2 Ion Exchangers

Ion exchangers are insoluble solid materials which carry exchangeable cations or anions. These ions can be exchanged for stoichiometrically equivalent amount of other ions of the same sign when the ion exchanger is in contact with electrolyte solutions. Carriers of exchangeable cations are called cation exchangers, carriers of exchangeable anions are called anion exchangers, and materials that are capable of both cation and anion exchange are called amphoteric ion exchangers.

Ion exchangers owe their characteristic properties to a peculiar feature of their structure. They consist of a framework which is held together by chemical bonds or lattice energy. This framework carries a positive or negative electric surplus charge which is compensated by ions of opposite sign, so-called counter ions. The counter ions are free to move within the framework and can be replaced by other ions of the same sign [1].

Many different natural and synthetic products show ion exchange properties. These can be generally summarized as ion exchange coals, mineral ion exchangers like crystalline alumosilicates including zeolites, synthetic inorganic ion exchangers resembling zeolites and synthetic organic ion exchange resins.

1.2.1 Ion Exchange Resins

The most important class of the ion exchangers are the organic ion exchange resins. Their framework, the so called matrix, consists of an irregular, macromolecular, three-dimensional network of hydrocarbon chains. The matrix carries ionic groups such as

$-SO_3^-$, $-COOH^-$, $-PO_3^{2-}$, $-AsO_3^{2-}$ in cation exchangers,

and

$-NH_3^+$ $=NH_2^+$, $=N^+=$, $\equiv S^+$ in anion exchangers [1].

The overall structures of these ion exchangers are illustrated in Figure 1.2.

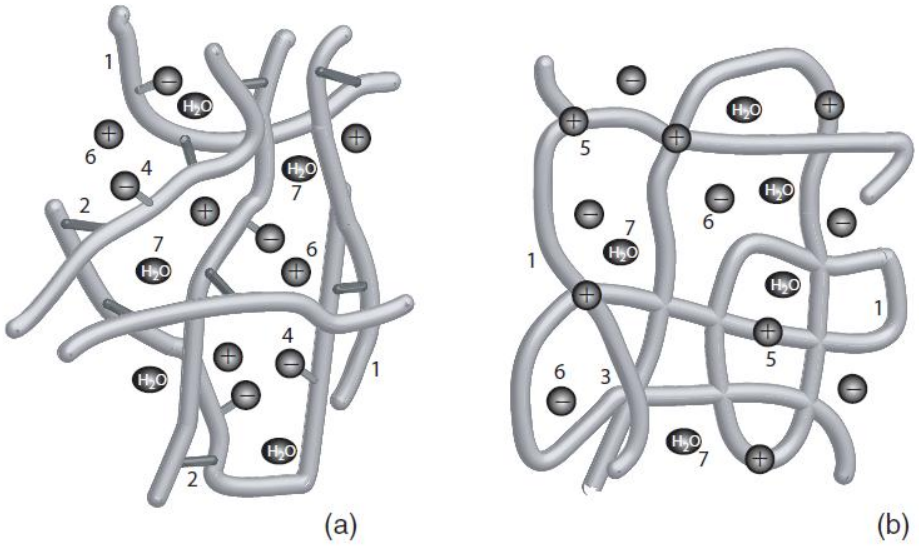

Figure 1.2 Schematic representations of polymeric ion exchangers. (a) Cross-linked cation exchange material; (b) Anion exchange materials with unrecognisable cross-links. 1–Polymeric chain; 2–cross-link; 3–physical knot; 4–negatively charged cation exchange group attached to the chain; 5–positively charged anion exchange group incorporated in chains; 6–counter ion; 7–water [2].

Ion exchange resins thus generally are crosslinked polyelectrolytes. The matrix of the resin is hydrophobic. However, hydrophilic components are introduced by incorporation of its ionic groups listed above. Ionic groups can be introduced during the polymerization of nonionic monomers or by introducing the functional groups after the polymer is formed.

Linear hydrocarbon molecules with ionic groups are soluble in water. The ion exchange resins, in contrast, are made insoluble by introducing of crosslinks which interconnect the hydrocarbon chains. Since the dissolution of an ion exchange resin particle, practically a single molecule, would require rupture of carbon-carbon bonds, the resins are insoluble in all solvents by which they are not destroyed. However, matrix is elastic and can be expanded. Hence the resins can swell by taking up solvents. The framework of the resins, in contrast to that of zeolites, is flexible and random network [1].

1.2.2 General Properties of Ion Exchange Resins

1.2.2.1 Functionality

Chemical properties of functional groups define the type of a particular ion exchange resin. Cation and anion exchangers are the two types bearing respectively the negatively and positively charged groups listed in Table 1.1 and, hence, are able to exchange cations or anions.

Table 1.1 Functional groups of ion exchange resins.

CATION EXCHANGERS		ANION EXCHANGERS	
Type	**Functional Group**	**Type**	**Functional Group**
Sulfonic acid	$-SO_3^- H^+$	Quaternary amine	$-N(CH_3)_3^+ OH^-$
Carboxylic acid	$-COO^- H^+$	Quaternary amine	$-N(CH_3)_2(EtOH)^+$
Phosphonic acid	$-PO_3^- H^+$	Tertiary amine	$-NH(CH_3)_2^+ OH^-$
Phosphinic acid	$-HPO_2^- H^+$	Secondary amine	$-NH_2(CH_3)_2^+ OH^-$
Phenolic	$-O^- H^+$	Primary amine	$-NH_3^+ OH^-$
Arsonic	$-HAsO_3^- H^+$		

In addition, due to different dissociation properties of these functional groups, strong and weak exchangers are recognized to be similar to that of strong and weak electrolytes. These four main types of ion exchange resins are;

1) Strongly acidic resins: Resins with sulfonic acid groups are these type of resins and the most typical example of ion exchange resins is sulphonated polystyrene crosslinked with divinyl benzene (Figure 1.3).

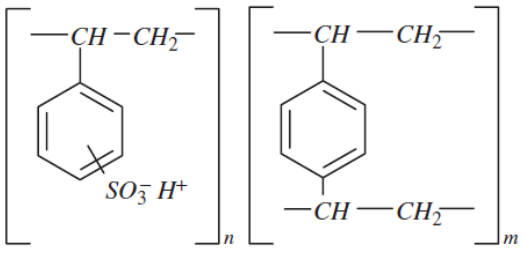

Figure 1.3 The structure of sulphonated polystyrene crosslinked with divinyl benzene [2].

Another common example of this type of resins is copolymers of phenol with formaldehyde (Figure 1.4).

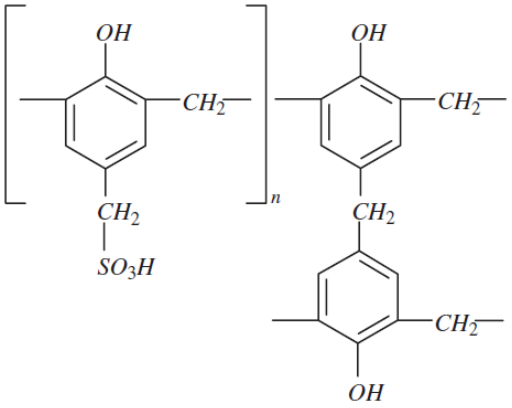

Figure 1.4 The structure of copolymers of phenol with formaldehyde [2].

2) Weakly acidic resins with carboxylic acid groups are these types of resins, and a variety of processes have been carried out for the preparation of these resins involving methacrylic acid, or maleic anhydride. Copolymers of polyacrylic or polymethacrylic acid with divinylbenzene shown in Figure 1.5 can be a common example.

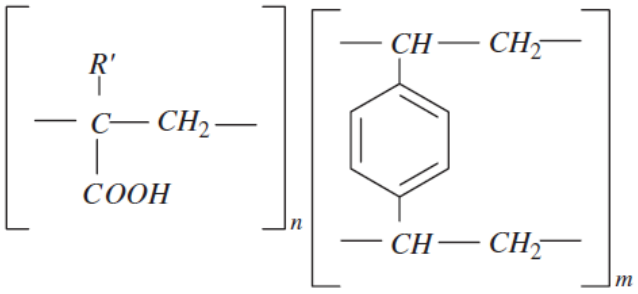

Figure 1.5 Copolymer of polyacrylic or polymethacrylic acid with divinylbenzene where R' is H in polyacrylic and R' is CH_3 in polymethacrylic polymers [2].

3) Strongly basic, (eg. resins with trimethylammonium groups)

4) Weakly basic (eg. resins with amino groups) [2].

1.2.2.2 Capacity

The capacity is defined as the number of functional groups available for a certain kind of an ion or maximum number of ions that can be accommodated by a certain amount of material [2] and is the most important property of an ion exchanger, since it permits a quantitative determination of how many counterions can be taken up by the exchanger.

The capacity depends on various conditions among which the influence of pH is the most important [4]. Partial or incomplete dissociation of weak acidic resins at low pH and that of weak basic resins at high pH and high selectivity of these resins in their behavior towards H^+ and OH^- ions make their capacity strongly dependent on the pH of the ion exchange medium. The capacity of the resins with strong acidic or basic group however, is naturally independent of pH [2, 4, 5].

The exchange capacity of a cation exchange resin is usually measured in the laboratory by determining the number of milligram equivalents of sodium ion which are sorbed by one gram of the dry resin in the hydrogen form [5].

1.2.2.3 Selectivity

The selectivity of an ion exchanger is defined as the property of a certain ion exchanger to exhibit a preferential activity for different ions or simply high affinity. The selectivity is influenced various factors including (1) exchangeable ions (size and charge); (2) properties of the exchanger i.e. particle size, degree of crosslinking, capacity, and type of functional groups; (3) nature of medium i.e. total concentration of as well as concentration ratio of the existing ions both capable and incapable of exchange, as well as the type and quantity of other substances in the solution; and (4) the reaction period [4].

For dilute solutions; of course there are exceptions, in the usual general-purpose cation exchangers the selectivity sequence of most common cations is approximately:
Fe^{3+}> Al^{3+} > Pb^{2+} > Sr^{2+} > Ca^{2+} > Ni^{2+} > Cd^{2+} >Cu^{2+} > Co^{2+} > Zn^{2+} > Mg^{2+}> Mn^{2+} > UO_2^{2+} >Ag^{+} > Cs^{+} > Rb^{+} > K^{+} > NH_4^{+}> ≈ Na^{+} > H^{+}> Li^{+} > Hg^{2+}
A corresponding list for anion exchangers is;
Citrate > SO_4^{2-} > oxalate > I^{-}> $NO3^{-}$ >CrO_4^{2-} > PO_4^{3-} > HSO_4^{-} > NO_3^{-} > Br^{-} > SCN^{-} > Cl^{-}> formate >acetate > F^{-} > ≈ OH^{-}
The places of the H^{+} and OH^{-} in these sequences are dependent on the strength of the functional group in exchanger [1].

1.2.2.4 Crosslinking

Crosslinking provides the fundamental chemical bonding between adjacent polymer chains thus giving the resin its inherent physical strength [3]. The density of crosslinks between polymeric chains is called degree of cross-linking. It influences the structure of the matrix, its elasticity, swelling ability of the material, and mobility of the counterions inside the exchanger. Materials with high crosslinking are hard, brittle and, in many cases, more stable. However, diffusion in such materials is slow causing reduction of the rate of all processes due to their increased sensitivity to osmotic influences [2, 4]. Exchangers with low degree of crosslinking can be even jelly-like and soft and mechanically unstable in swollen state. Their stability could be low in benefit of fast kinetics of interactions [2].

1.2.2.5 Physical Structure of Ion Exchange Resins

As mentioned before, ion exchange resins consist of an essentially irregular macromolecular, three-dimensional network of hydrocarbon chains bearing functional groups. The matrix and functional groups define the chemical properties of the polymer. However, besides the chemical structure, physical configuration of the

material is also highly important for the performance, because it defines surface area, mechanical stability, resistance to a liquid flow, etc. Even thermodynamic and kinetic characteristics of ion exchange are dependent on the macrostructure of the material.

Ion exchange polymers differ due to differently distributed density of the gel;

- *The gel resins* (**a** in Figure 1.6 and Figure 1.7) have relatively homogeneous polymer density across the bead. The gels have no well-defined pore structure; however, the molecular and nano-scale open areas between the hydrocarbon chains are conventionally designated as pores without considering the true geometry. When the gels are swollen, these pores contain the solvent; the pores collapse at drying and are thus virtually non-existent in dry state.
- The *isoporous resins* (**b** in Figure 1.6 and Figure 1.7) have specially designed homogeneous distribution of polymeric chains across the bead and thus more regular structure of the micropores.
- The macroporous resin (**c** in Figure 1.6, Figure 1.7 and Figure 1.8) which are the most widely used materials nowadays (also called as macroreticular in literature) have heterogeneous (in nano- and macro-scale) structure consisting of two phases: (1) gel regions containing dense polymer chains and a minor amount of the solvent, 2) macroscopic permanent pores containing solution similar to the surrounding medium [2].

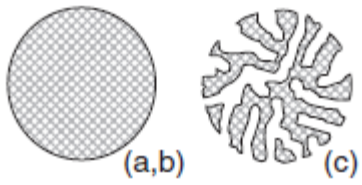

Figure 1.6 Morphology of ion exchangers: (a) gel resins; (b) isoporous resins; (c) macroporous resins.

Figure 1.7 Distribution of polymeric chains in ion exchangers: (a) gel resins; (b) isoporous resins; (c) macroporous resins.

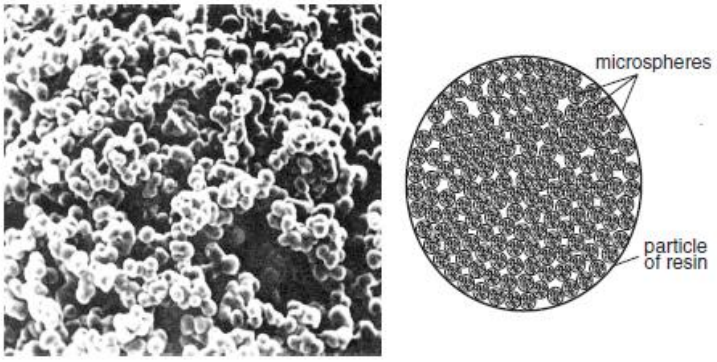

Figure 1.8 Illustration of the macroreticular resin and micrograph of macroporous resin [2].

In the light of all these; in synthesizing an ion exchange resin, several basic requirements must be taken into consideration.

- The resin must be sufficiently cross-linked but a negligible solubility.
- The resin must be sufficiently hydrophilic to permit diffusion of ions through the structure at a finite and usable rate.
- The resin must contain a sufficient number of accessible ion exchange groups.
- The resin structure must be chemically stable.
- The resin must be physically stable in terms of mechanical strength and resistance to attrition.
- The resin must have thermal stability.
- The resin must have controlled and effective exchange capacity.
- The resin must have consistent particle size and effective surface area compatible with its planned usage [3].

1.2.3 Application of Ion Exchangers

The list of some conventional and prospective applications of ion exchange resins can be presented below as;

- Softening of water.
- Purification of water.
- Deionization of water.
- Separation of uranium isotopes, waste decontamination, final storage of radioactive wastes, condensate polishing in nuclear industry.
- Decontamination and recuperation of waste streams.
- Recovery and purification of biological and biochemical substances.
- Isotope separation.
- Removal of inorganic salts from liquors in pulp and paper industry
- Purification of sugars and polyhydric alcohols
- Deacidification of fruit juice, recovery of glutamic-acid, removing off tastes and odours in food industry.
- Extraction of lactoperoxidase, lactoferrin and purification of casein in dairy
- Adsorption of wine proteins in the production of wines and stabilisation of wine in winery.
- In biotechnology.
- Recovery of uranium, thorium, rare earths, tungsten, transition metals, gold, silver, platinum, palladium, and purification in hydrometallurgy.
- Solvent purification.
- Reagent purification.
- Pharmaceutics and medicine.
- Evaluation of soil properties, remediation of contaminated soils, artificial soils in soil science and technology.
- As permaselective membranes [2].

1.3 Polypropylene

Polypropylene was first produced by G. Natta, following the work of K. Ziegler, by the polymerization of propylene monomer (Figure 1.9) in 1954. The steric arrangements of the methyl groups give stereochemistry of the PP chain [6, 7]. Polypropylene can be in the form of (*i*-PP), syndiotactic (*s*-PP), and atactic (*a*-PP) depending its stereoregularity (Figure 1.10).

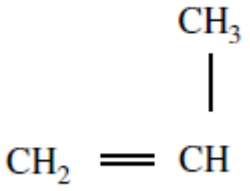

Figure 1. 9 Propylene monomer.

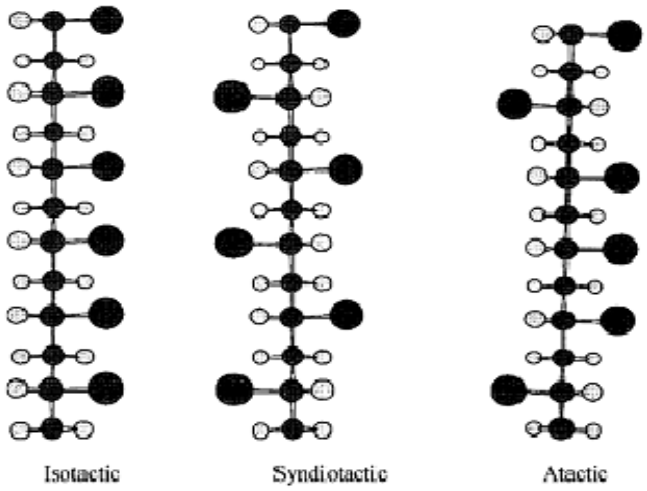

Figure 1.10 Structures of isotactic, syndiotactic and atactic polypropylenes [8].

Depending on their structures, they have different properties. The mostly used polypropylene is the isotactic polypropylene [9] which has the ordered rearrangement of methyl group at the same side of the chain [8]. In Isotactic polypropylene, methyl

groups force the chain to prefer helical conformation. As a result of the ordered helical conformation, isotactic polypropylene crystalizes easily [10].

In the crystalline state, isotactic polypropylene prefers an alternate trans and gauche (TGTGTG....) conformation with respect to main chain carbon atom. This conformation results in a three fold (31) symmetry of helix with a chain repetition of 6.50 Å as shown in Figure 1.11 [11].

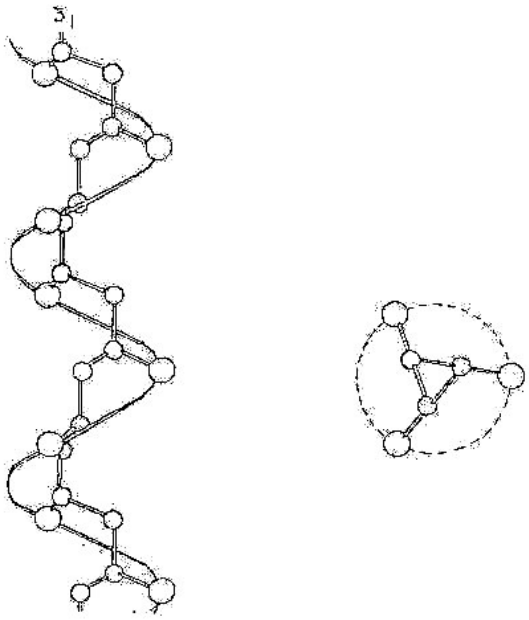

Figure 1.11 The 3_1 helical conformation of isotactic PP in crystalline state [7].

The wide use of isotactic polypropylene as a practical solid material is undoubtedly due to its high crystallinity. It shows polymorphism due to crystallization into a variety of modification of different orders. The crystal structures of isotactic polypropylene have been studied extensively and were recognized to be influenced by various conditions of polymer processing, such as, heating temperature to melt, and cooling rate from the melt to the solid state. As the tacticity along the polymer chain

is reduced, the crystallinity decreases. In the extreme case, the crystallinity of atactic PP is practically zero [12].

Atactic polypropylene is obtained as a byproduct during synthesis of isotactic polypropylene [13]. Although isotactic polypropylene is rigid solid, atactic polypropylene is a soft and disordered material with low degree of crystallinity [10].

Polypropylene is one of the widely used polymeric materials due to its mechanic, physical and thermal properties with its high melting point, low density and good impact resistance [14]. However, the use of PP is limited in several industrially important fields particularly due to lack of chemical functionalities, sensitivity to photo or thermal oxidation, its low surface energy, difficulty in dyeing, extremely poor hygroscopicity, low strength and modulus, low melting and sticking temperature, inadequate compatibility with other synthetic polymers, and virtually no adhesion to metal and glass. Chemical modification of PP by introduction of functional groups improves its commodity of this polymer. This modification is made by copolymerization of propylene with polar monomers or by grafting or graft copolymerization of functional compounds to the PP backbone, and reinforcement of PP by fibers, and its importance are still in progress today [15].

The modification of polyolefins, particularly polypropylene, by functionalizing to obtain engineering materials with superior properties, has been the area of interest shared with several workers in recent years. Functional and engineered polyolefins are becoming more and more commercially important and expanding their application [16].

The modified properties of polymers by grafting or copolymerization result in increased intermolecular interactions and possible crosslinking of the macromolecules. The surface chemistry and physics of polymers can also be altered

by several surface modifying techniques such as surface coating, degradation, hydrolysis, and radiation induced, photochemistry-induced, or catalytic-initiated graft copolymerization. On the other hand, modification of polymers through graft copolymerization may introduce some desirable properties into the polymer without a change in the architecture of the polymer backbone and thus gives rise to commercial importance for polymer applications. Grafting improves adhesion, stability, and compatibility for required engineered polyolefin composites [17].

1.4 Modification of Polypropylene

The design and development of sorption-active natural and synthetic resins, membranes, fibers and textile materials is of great scientific and practical interest. The advantages of that type of polymeric adsorbents, such as their highly developed specific surface, excellent ion-exchange parameters and ease of use especially under continuous conditions, allow them to find a great application in the chemical, biomedical, ecological and industrial fields [18].

Various approaches to synthesize ionically active polypropylene adsorbents have been developed, including direct graft polymerization of vinyl monomers already containing desirable chemically active functional groups or graft copolymerization of two (or more) different types of monomers onto polymer backbone and graft polymerization of a precursor-monomer which can be subsequently modified [19, 20, 21]. Owing to limited number of vinyl monomers with functional groups, latter approaches are considered as the most perspective ones. There are numerous publications on grafting of glycidyl methacrylate on PP and subsequent ring opening of the epoxy groups and functionalization with various reagents, such as amines and hydroxylamine [22, 23], sulfuric acid [24], phosphoric acid [25], iminodiacetic acid [26], sodium sulfite [27] and amino acids [28].

There are also other studies generally based on grafting of acrylic acid [29], acrylamide [30, 31], sulfonate glycidyl methacrylate [32, 33] onto PP and graft copolymerization of sulfonated polystyrene with PP [34].

In recent years, grafting of polar monomers, like maleic anhydride (MAH), on polyolefin has also attracted great attention. The polar groups introduced may increase the ability to funtionalize and so increase the compatibility and the special interactions and lead to the formation of adhesion of the polyolefin [35]. The graft polymerization of MAH onto PP in the presence of a radical initiator is probably the simplest, most widely used method, especially with peroxide initiators. There are many works focusing on the grafting on PP, in both solution-state [36, 37], melt-state [38-40] and solid-state graft polymerization [41-43].

1.5 Melt Grafting of Maleic Anhydride on to Polypropylene

The functionalization of polypropylene through grafting unsaturated monomers such as maleic anhydride (MA) in the presence of organic peroxide as an initiator, has received much attention over the past decades. Functionalized PP has been prepared successfully by using solution [44, 45], melt [46-49] and solid state routes [50-52]. The modified PP has been used extensively for compatibilization of immiscible polypropylene-polyamide and polypropylene-polyester blends, as well as to improve the interfacial adhesion of PP with glass and carbon fibers, and even as a processing aid for degradable plastics [53, 54]. In spite of the commercial success of functionalized polyolefins, the precise nature of the chemical paths involved in the functionalization process is not completely clear. It is generally accepted that chain scission occurs during the peroxide initiated functionalization of PP [48]. One of the possible reaction mechanism proposed for the grafting of MA onto the PP is given in Figure 1.12.

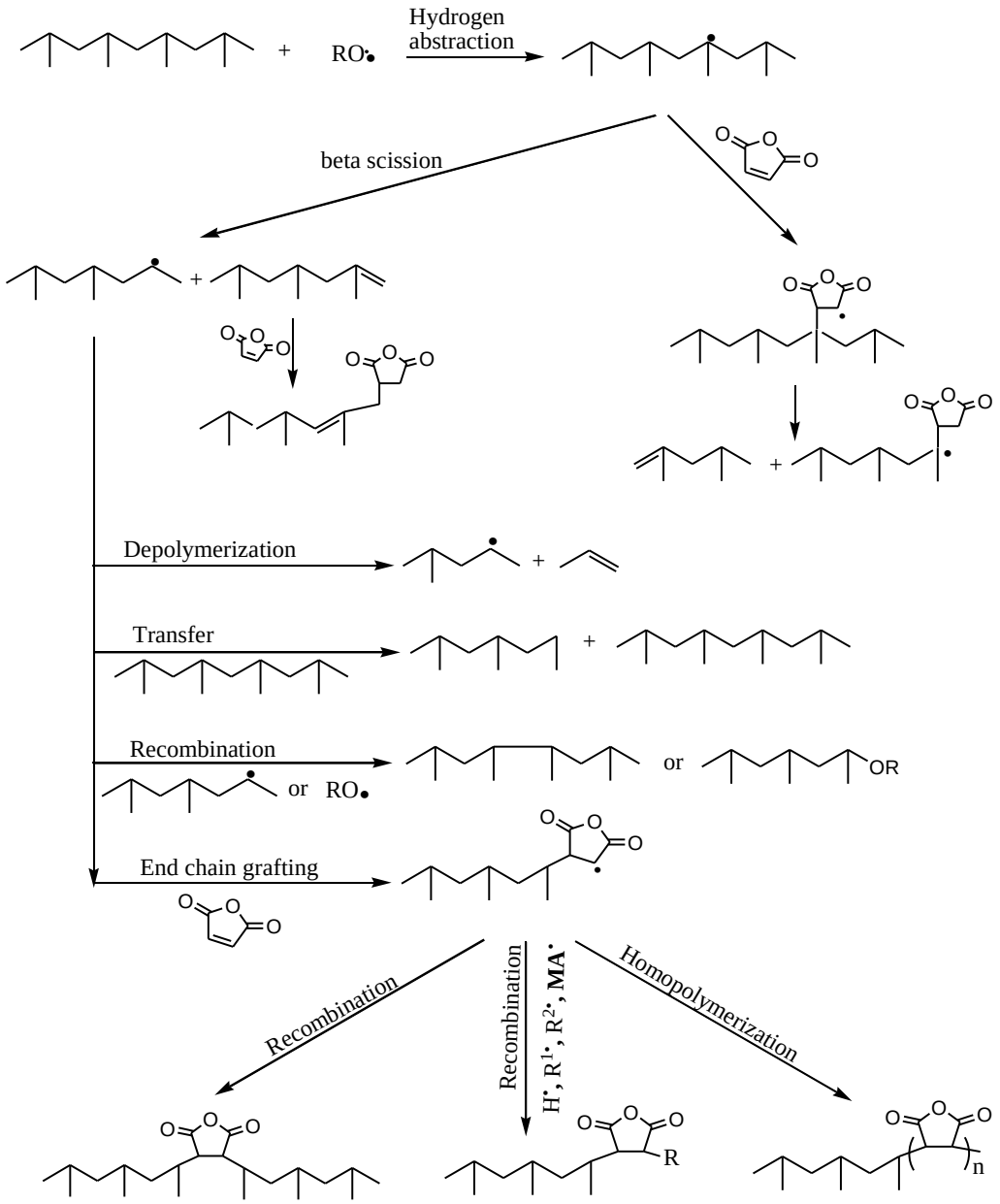

Figure 1.12 The possible reaction mechanism for the grafting of MA onto the PP [55].

In an earlier study using a solution grafting process, it was proposed that the graft reaction involved mainly the appending of MA to tertiary carbons along the PP backbone [45]. Another study, in which the grafting reaction was performed by means of melt grafting process, suggested that MA might be appended to tertiary site

along the PP backbone as a single ring or as short branches that were attributed to homopolymerization of MA [48]. More recently, the probability of the homopolymerization of MA that can take place during the processing was also reported [44]. However, it was also pointed out in some studies that according to the ceiling temperature, there is no possibility for the homopolymerization of MA to occur under the melt grafting process conditions (at 190ºC) [56, 57]. It is also indicated that the grafted MA might also introduce cross-links between the PP chains [50]. There were also some findings about the MA-g-PP materials that consist of single anhydride rings connected to the PP chain ends [58].

From the aforementioned studies, although it can be noted that the grafting reaction mechanisms of MA-g-PP proposed by several researchers are somehow controversial, the main reactional path for the grafting of PP with MA can be given as in Figure 1.13.

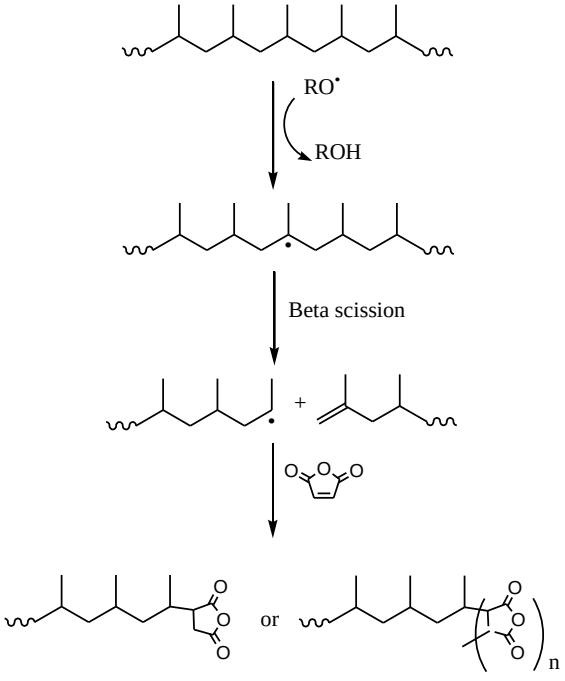

Figure 1.13 Main reactional paths for the grafting of PP with MA [59].

In general the reaction of maleic anhydride with molten polypropylene in the presence of a peroxide initiator is processed as a heterogeneous reaction accompanied by chain scission and/or degradation reaction, and it is possible to produce MA-g-PP materials with low molecular weights.

1.6 Peroxide Crosslinking of Polypropylene

There have been number of works published in which the crosslinking of polypropylene was initiated by thermal decomposition of peroxide [60-65]. According to these studies, polypropylene can possibly be crosslinked, but crosslinking process is complicated, because of the presence of simultaneous chain scission.

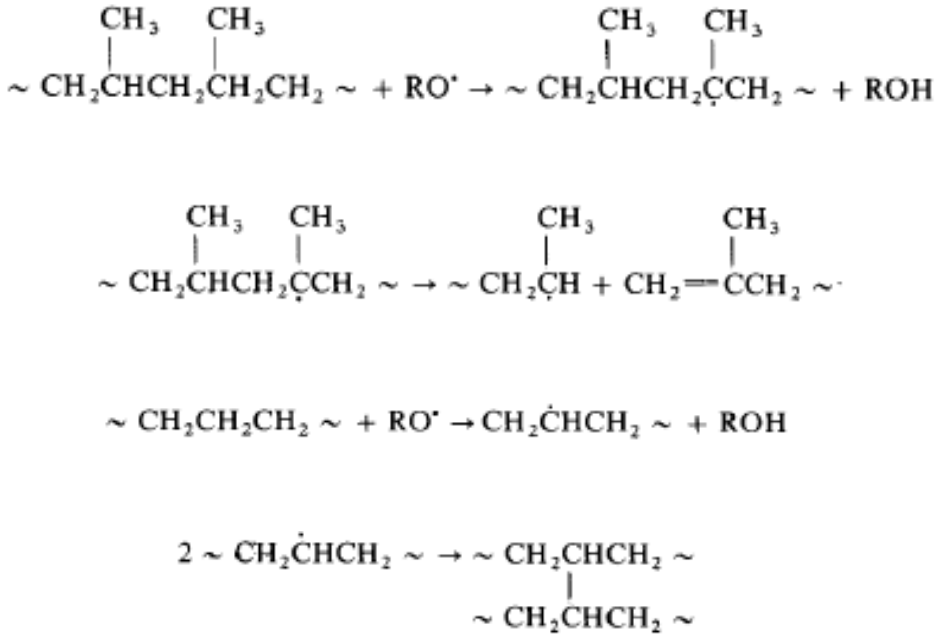

Figure 1.14 Scission and crosslinking of polypropylene.

It is also well established that chain scission leads to a decrease in molecular weight and a narrow molecular distribution [66-68]. It is also found that although this process is often accompanied by crosslinking and branching, efficiency is low to give a measurable level of gel [69]. The efficiency of crosslinking depends on the decomposition rate of peroxide and reactivity of the radicals formed. It was observed that initial gelation rate increases linearly with peroxide concentration and temperature, and at high peroxide concentration levels. However significant β-scission and other side reactions occurs simultaneously [70]. Influence of crosslinking temperature also shows that efficiency increases with decreasing temperature [64].

1.7 Aim of the study

In this study, to synthesize polypropylene based ion exchange resin we aimed to;

- synthesize maleic anhydride-g-polypropylene (MA-g-PP) by melt grafting of maleic anhydride (MAH) on to polypropylene to functionalize PP,
- neutralize MA-g-PP samples with different metal salts to give MA-g-PP an ionic character,
- peroxide crosslinking of neutralized MA-g-PP samples to gain physical and chemical stability,
- characterize the chemical and physical structure of prepared resins with spectroscopic methods,
- test the prepared resins to observe whether they have ion exchange characterot not.

CHAPTER 2

EXPERIMENTAL

2.1 Materials

Isotactic Polypropylene (MH453 Petkim), Maleic Anhydride (Merck), Dicumyl Peroxide (Merck), KOH (Merck), o-Cresolsulfonephthalein (cresol red) (Merck), Thymolphthalein (Merck), Ethanol (J. T. Baker), Xylene (Merck), Trichloro Acetic Acid (Riedel-De-Hen), NaOH (Merck), $Ca(C_{17}H_{34}COO)_2$ (Merck), $Mg(C_2H_3O_2)_2.4(H_2O)$ (Merck), KOH (Merck), Sodium Acetate Trihydride (Merck), Potassium Acetate (Merck), Acetic Acid Glacial (Merck), Nitric Acid (HNO_3) (Merck), Potassium Hydrogen Phthalate (KHP) (Merck), Sodium Carbonate (Na_2CO_3) (Merck), $Cu(NO_3)_2$ (Merck), $Co(NO_3)_2$ (Merck), $Cd(NO_3)_2$ (Merck), $Co(NO_3)_2$ (Merck), $Pb(NO_3)_2$ (Merck), $Fe(NO_3)_3$ (Merck), technical acetone and technical ethanol were used as received.

2.2 Instrumentation and Method

2.2.1 Mixing

The grafting of MA onto PP was peformed by melt mixing in a Brabender Plasti-Coder Torque Rheometer model PLV 151 (in Figure 2.1 and Figure 2.2). The capacity of Brabender is 50 ml.

Figure 2.1 Brabender Plasti-Coder Torque Rheometer model PLV 151.

The mixing chamber was heated by circulating oil and a thermometer was used to monitor the oil temperature.

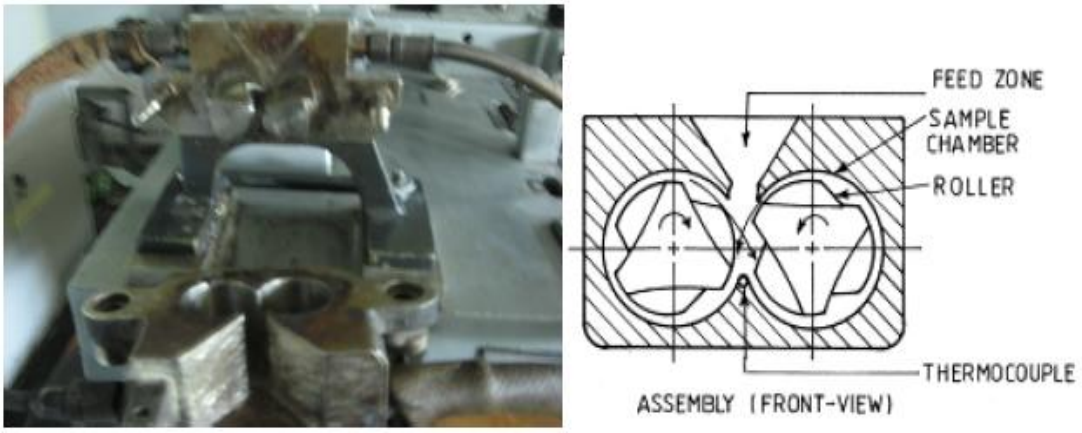

Figure 2.2 Schematic diagram of an internal roller mixer.

2.2.2 Melt Flow Index (MFI)

The Melt Flow Index (MFI) is defined as the weight of the material extruded in specified time through a capillary of specific diameter and length by pressure applied through dead weight under prescribed temperature conditions [71]. MFI test was performed in order to determine the flow behavior of the samples, which is inversely related to melt viscosity. For linear polymers, the melt flow rate is also used for an indirect measure of molecular weight, high melt flow rate corresponding to low molecular weight [72]. In this study, Coesfield Material Test, Meltfixer LT (Figure 2.3) was used for the test.

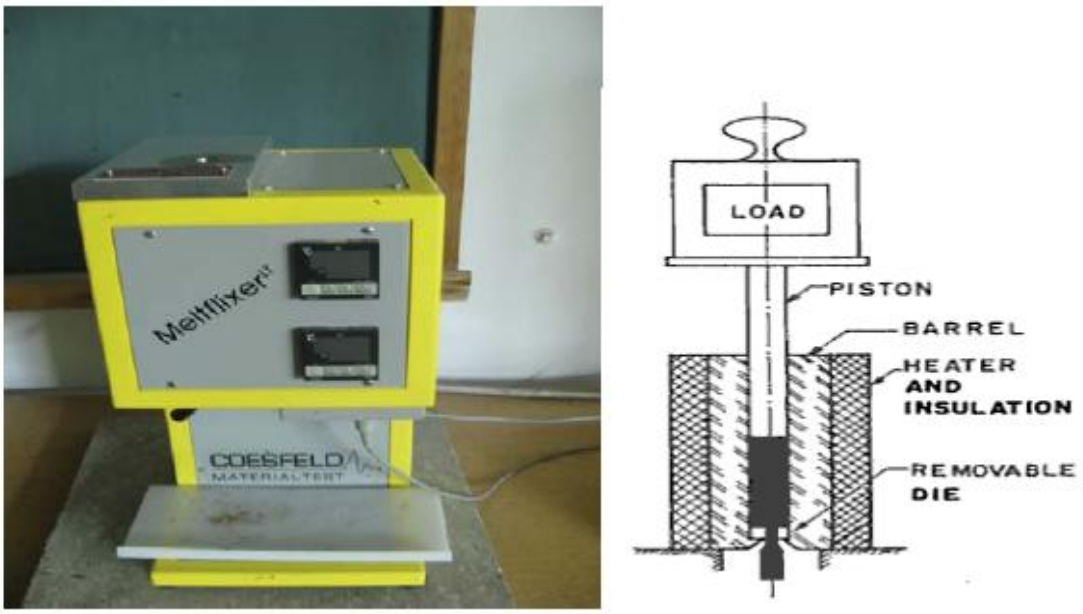

Figure 2.3 Melt Flow Index instrument.

2.2.3 Attenuated Total Internal Reflection (ATR) Infrared Micro Spectroscopic Imaging System

Infrared spectroscopy (FTIR) spectra of the samples were recorded with a Bruker Vertex 70 spectrometer.

2.2.4 Scanning Electron Microscopy (SEM)

The Scanning Electron Microscopy is a type of electron microscope capable of producing high-resolution images of a sample surface. Due to the manner in which the image is created, SEM images have a characteristic three-dimensional appearance and are useful for judging the surface structure of the sample.

In this study, SEM at METU Central Research Laboratory was used to analyze the morphologies of samples. The images were magnified x20000-x40000.

2.2.5 Scanning Electron Microscopy-Energy Dispersive X-ray Spectroscopy (EDX)

In this study, to characterize the metal ion components of the neutralized MA-g-PP resins, SEM-EDX analysis was done at METU Central Research Laboratory.

2.3 Characterization of Ion Exchange Properties

2.3.1 Batch Equilibrium Method

Ion exchange processing can be accomplished by either a batch method or a column method. While column procedures are preferred in industry, batch operations are rarely used in industrial process, but they are well-studied for laboratory purposes due to their simplicity of the experimental setup [2, 73-79]. In this method; ion exchanger is contacted with the electrolyte solution of any desired vessel until exchange equilibrium has been established between the counter ions of the exchanger and the ions of the equal charge of the electrolyte. After equilibrium has been attained, the ion exchanger is filtered [4]. Then ion content of filtrate is quantified either by instrumental [76-79] or analytical methods [73-75].

2.3.2 Atomic Absorption Spectoctroscopy

Unicam 929 Model Atomic Absorption Spectroscopy was used to measure metal ion concentration of the filtrate solutions after batch equilibrium method to characterize the metal ion uptake of the resins prepared.

2.4 Experimental Procedure

2.4.1 Melt Grafting of Maleic Anhydride onto Polypropylene

The melt grafting of MA onto PP in the presence of dicumyl peroxide (DCP) was carried out in the Brabender Plasticorder at 195-200^{o}C at a rotor speed of 60 rpm

under a nitrogen atmosphere. Table 2.1 represents the reaction compositions (C) of samples studied.

Table 2.1 The reaction compositions of grafted samples.

Sample no	$C_{(DCP)}$ (phr*)	$C_{(MA)}$ (phr*)
1	0	0
2	0.25	0.50
3	0.25	1.00
4	0.25	2.50
5	0.25	5.00
6	0.50	0.50
7	0.50	1.00
8	0.50	2.50
9	0.75	0.50
10	0.75	1.00
11	0.75	2.50

* phr = parts per hundred resin

DCP and MA were ground into powder before mixing with PP. PP (100 parts by weight) loading was first introduced into the mixing chamber and premelted for 4 minutes. After 4 minutes, MA and DCP were introduced simultaneously. The reaction mixture was mixed for additional 6 minutes.

2.4.2 Purification

The MA-g-PP samples were dissolved in hot xylene and then precipitated by technical ethanol. After the filtration, samples were washed with ethanol and acetone several times for the elimination of the unreacted MA monomer or possible MA oligomers formed during the grafting process described previously [80].

2.4.3 Determination of the Maleic Anhydride Content of the MA-g-PP by Volumetric Titration

1 g of MA-g-PP was dissolved completely in 200 mL of boiling xylene at about 120^{o}C. The mixture was refluxed for half an hour for the complete dissolution of the samples. After dissolution, 0.2 mL water was added and refluxed for another 1 h to hydrolize all anhydride functions. Afterwards 10 mL of 0.05 M KOH of ethanol solution was added dropwise and the mixture was refluxed for another 2 h to ensure complete reaction of KOH with the maleic anhydride (MA) groups. With the ethanolic solution of o-cresolsulfonephthalein as an indicator, the hot solution was back titrated with 0.03 M trichloro acetic acid of ethanol solution. A blank solution (for pure PP) was also treated under the same conditions. The grafting degree G (wt %) of the MA onto PP was calculated by the equation;

$$G = \frac{M(V_0 - V)M_0}{2 \times W \times 1000} \times 100\% \quad (3)$$

where;

M is the acid concentration of the ethanolic trichloro acetic acid solution (mol/L),

W is the weight of the MA-g-PP (g),

V_0 is the volume (mL) of the ethanolic trichloro acetic acid solution added to the blank solution during the titration,

V is the volume (mL) of the ethanolic trichloro acetic acid solution added to MA-g-PP during the titration,

M_0 is the molecular weight of MA (98.06 g) [32, 41, 47, 81, 82].

2.4.4 Melt Flow Index

MFI measurements of the MA-g-PP samples were carried out at 190°C, with a standard load of 2.16 kg. After the placement of test samples, standard weight was placed on the piston of the instrument to compress the sample. The molten grafted PP started to flow from the orifice of MFI. The mass of grafted PP was determined and recorded in grams/10 sec (g/10 sec).

2.4.5 Neutralization of the MA-g-PP with Metal Salts

MA-g-PP was dissolved in xylene and neutralized by adding ethanol solution of NaOH, $Ca(C_{17}H_{35}COO)_2$, $Mg(C_2H_3O_2)_2.4(H_2O)$ and KOH drop wise, for individual cations. And the mixture was refluxed for 4 h under a nitrogen purge. Each ionomer was precipitated in acetone, collected, washed with ethanol several times and dried at 60^oC for 24 h [17].

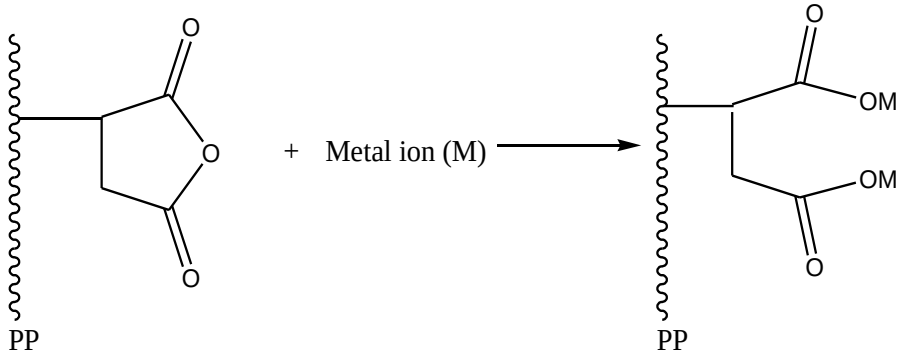

Figure 2.4 Neutralization reaction of MA-g-PP with metal salts where M represents the Na^+, K^+, Ca^{2+} an Mg^{2+} ions in this study.

2.4.6 Characterization of Neutralized MA-g-PP Samples by ATR

Characterization of the MA-g-PP and neutralized MA-g-PP samples were done by Attenuated Total Internal Reflection (ATR) Infrared Micro Spectroscopic Imaging System. In order to characterize the grafted maleic anhydride groups, purified MA-g-PP samples were pressed into films by compression moulding machine at 200°C and submitted to heat treatment at 130°C for 24 h to convert the possible acid groups to anhydrides by [83].

2.4.7 Crosslinking of Neutralized MA-g-PP samples

Peroxide cross-linking of Na^+, Ca^{2+}, Mg^{2+} and K^+ neutralized MA-g-PP samples was carried out in an oil bath. Samples and the 10 phr dicumyl peroxide were ground separately and mixed mechanically before the process. In the presence of small amount of xylene, reaction mixture is heated at 150-155°C for 10 half-life times of dicumyl peroxide (for about 45 min) under N_2 atmosphere. The mixture was then let cool down to 80°C under N_2 atmosphere again. The cross-linked resin was collected by precipitating in the small amount of acetone and then dried at 80°C for 24 hr.

2.4.8 Characterization of Crosslinked Resins

2.4.8.1 Swelling Index Determination

The specimens of Na^+, Ca^{2+}, Mg^{2+} and K^+ neutralized resins of known weights were immersed in xylene and acetone separately for 12 hours at room temperature. The samples were then removed from xylene and acetone, wiped with tissue paper to

remove excess liquid from the surface, and weighed. The swelling index of the resins was calculated as follows [84]:

$$Swelling\ index = \frac{W_2}{W_1} 100\% \quad (4)$$

where;

W_1: weight of the specimen before immersion

W_2: weight of the specimen after immersion.

2.4.8.2 Gel Content Determination

The percent gel contet of cross-linking in Na^+, Ca^{2+}, Mg^{2+} and K^+ neutralized resins was measured according to the weight loss after 14 hr soxhlet extraction of samples in boiling xylene. The samples were dried at 80 °C and subsequently weighed. The percentage of gel content was calculated as follows [84]:

$$\%\ gel\ content = \frac{W_g}{W_0} 100\% \quad (5)$$

where

W_g : weight of the sample after extraction

W_o : weight of the sample before extraction.

2.4.9 Morphological Analysis

2.4.9.1 SEM

Metal ion neutralized MA-g-PP resins, in the powder form, before and after crosslinking process were examined for their morphology by SEM.

2.4.9.2 SEM-EDX

The metal ion components of the metal ion neutralized MA-g-PP resins were characterized by SEM-EDX analysis. Before analysis, resins which were in the form of powder, were cold pressed to increase scanned surface for metal element investigation and dried at 90ºC-100ºC for two days.

2.4.10 Characterization of Ion Exchange Properties

In this work, ion exchange property of Na^+, Ca^{2+}, Mg^{2+} and K^+ neutralized MA-g-PP resins was investigated by batch equilibrium method. In all experiments, the resin samples used were in powder form.

2.4.10.1 Determination of the Ion Exchange Capacity of MA-g-PP

For the determination of the total acid capacity of the MA-g-PP resin (H^+ form of resin), it was firstly dried to constant weight at 100 ± 5 ºC. About 0.5 g of dry resin was accurately weighed into a conical flask containing10 mL of distilled water. 10 mL of 1 N NaOH was added. The flask was then closed with a stopper and let to stand for 4 hours with occasional stirring. The content of the flask was then back

titrated with 0.5 M HCl using thymolphthalein as an indicator. Before this procedure, prepared NaOH and HCl solutions were standardized with solution of Potassium Hydrogen Phthalate (KHP) and sodium carbonate (Na_2CO_3) respectively [3].

Capacity of the resin then was calculated as follows:

$$Capacity\ (meqg^{-1}) = \frac{10M_1 - M_2T}{W} \quad (6)$$

Where;

W: weight of dry resin

M_1: molarity of standard NaOH

M_2: molarity of HCl

T: titre of standard HCl (mL)

2.4.10.2 Evaluation of Metal Uptake at Different pHs

Sorption properties of non-neutralized MA-g-PP resin and the Na^+, Ca^{2+}, Mg^{2+} and K^+ neutralized MA-g-PP resins towards Cu^{2+}, Co^{2+}, Cd^{2+}, Pb^{2+} and Fe^{3+} ions at different pHs of 3, 4, 5 and 6 were studied. The study was restricted up to maximum pH=6, due to hydrolysis of metal ions at higher pH. The formation of metal hydroxide interferes with the ion exchange process.

The resin samples (0.5 g) were suspended in 50 ml of solution of metal ion with a concentration of 20 ppm, and the pH of the solution was adjusted with acetate buffers prepared by mixing following solutions of composition given in Table 2.2.

Table 2.2 Composition of acetate buffer solutions

pH	volume of 0.1M acetic acid solution	volume of 0.1M sodium acetate* solution
3	982.3 ml	17.7 ml
4	847.0 ml	153.0 ml
5	357.0 ml	643.0 ml
6	52.2 ml	947.8 ml

* For Na^+ neutralized resin, acetate buffer solutions were prepared with 0.1M potassium acetate solution instead of sodium acetate solution to prevent the common ion effect on ion exchange.

The suspension was stirred for a period of 12 hours at room temperature (incubation period). The resin was separated by filtration and the metal concentration in the solution was measured by AAS method on Unicam 929 spectrometer with a wavelength set at 324.8, 228.8, 232.0, 238.3 and 248.3 nm for Cu^{2+}, Cd^{2+}, Co^{2+}, Pb^{2+} and Fe^{3+}, respectively.

For the measurement on AAS, the standard solutions of Cu^{2+}, Co^{2+}, Cd^{2+}, Pb^{2+} and Fe^{3+} ions, having concentrations of 2 ppm, 5 ppm, 10 ppm, 20 ppm and 30 ppm, 40 ppm, 60 ppm, 70 ppm were also prepared from the 1000 ppm stock solutions of these four ions to plot calibration curves.

The quantity of the metal ions uptaken per unit of dry weight of the resin (mg/g) was calculated as follows [77, 85];

$$Metal\ ion\ uptaken = \frac{(C_0 - C_1)V}{W} \qquad \textbf{(7)}$$

where C_0 and C are the metal ion concentrations in the solution (mg/ml) before and after incubation period respectively, V is the incubation volume of the solution (ml) and W is the weight of the resin (g).

2.4.10.3 Evaluation of the Concentration Effect on Metal Uptake

In order to investigate the possible effect of the concentration of the solution in which resin is incubated on the uptake, Ca^{2+} neutralized MA-g-PP resin was incubated in 40 ppm, 60 ppm and 70 ppm solutions of Pb^{2+} ion separately for 12 hours. After the filtration of the resin, filtrate solutions were investigated for Pb^{2+} ion concentration by AAS.

2.4.10.4 Evaluation of Rate of Metal Uptake

In order to estimate the time required to reach the state of equilibrium under given pH, resins were subjected to metal ion solution at pH=6, for 10 hours at room temperature and metal uptakes were determined at certain time intervals.

2.4.10.5 Regeneration Evaluation

The reconversion of an ion exchanger into its working form is known as regeneration [4]. In order to find out the extent of reuse of the resins, filtered resin samples were dried and treated with 0.1 M HNO_3 solution for 8 hr at room temperature by continuous stirring. The resins were then refiltered and the filtrates were examined for released metal ions by AAS measurement.

CHAPTER 3

RESULTS AND DISCUSSION

3.1 Determination of the Maleic Anhydride Content of the MA-g-PP by Volumetric Titration

Purified MA-g-PP samples were titrated for the determination of maleic anhydride content. Grafting degree of the samples are listed and shown below:

Table 3.1 Maleic anhydride content of MA-g-PP samples

MA-g-PP samples	**$C_{(DCP)}$** (phr)	**$C_{(MA)}$** (phr)	**Wt % MA**
1	0.25	0.50	1.67
2	0.25	1.00	1.54
3	0.25	2.50	1.50
4	0.25	5.00	1.47
5	0.50	0.50	0.66
6	0.50	1.00	1.77
7	0.50	2.50	1.82
8	0.75	0.50	1.86
9	0.75	1.00	1.71
10	0.75	2.50	1.86

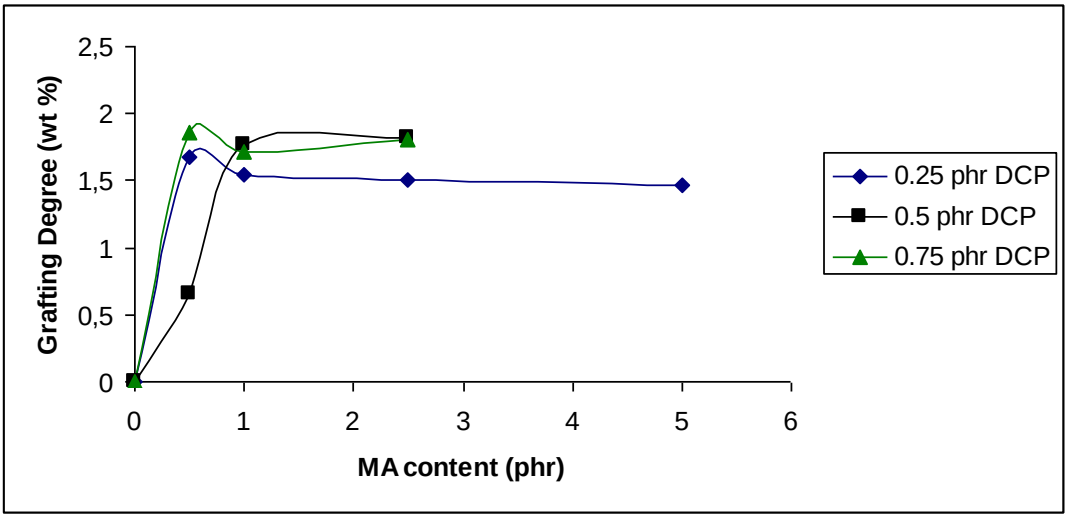

Figure 3.1 Grafting degree of MA-g-PP as a function of loading concentration of MA.

Degree of grafting of MA increases initially, reaches a maximum and then slightly declines. At a given concentration of DCP, when the loading concentration of the MA monomer is low, there are enough initial radicals to react with the MA monomer and initiate PP macroradicals (as shown in Figure 1.3). Therefore the grafting degree of PP is increased. Yet, it is assumed that further increase in the MA concentration, the most of the radicals would be consumed by MA. So the number of the initial radicals to induce grafting of MA onto the PP would decrease. This trend was also explained by the decarboxylation of the MA monomer on contact with the molten PP [17, 59, 86]. Our results and the trend observed in this work is in a good agreement with the literature given above.

3.2 Melt Flow Index

MFI measurements of the MA-g-PP samples were carried out at 190°C and 2.16 kg. Table 3.2 represents the MFI of MA-g-PP samples prepared.

Table 3.2 MFI of MA-g-PP samples prepared

MA-g-PP samples	**$C_{(DCP)}$** (phr)	**$C_{(MA)}$** (phr)	**Wt % MA**	**Melt Flow Index** (g/10sec)
PP	0.00	0.00	0.00	**0.14**
1	0.25	0.50	1.67	**1.38**
2	0.25	1.00	1.54	**1.37**
3	0.25	2.50	1.50	**1.31**
4	0.25	5.00	1.47	**0.80**
5	0.50	0.50	0.66	**1.48**
6	0.50	1.00	1.77	**2.19**
7	0.50	2.50	1.82	**2.52**
8	0.75	0.50	1.86	**1.50**
9	0.75	1.00	1.10	**1.11**
10	0.75	2.50	1.86	**1.29**

It is clearly seen from the higher MFI values of the MA-gPP samples compared to that of PP that how grafting process affects the molecular weight of the samples as a result of inevitable chain scission and/or degradation reaction that occurred during the grafting process. It is also seen that the increased initial maleic anhydride concentration did not cause an increase in the grafting degree however decrease in the MFI was observed for the constant peroxide concentration of 0.25 and 0.75 phr. This was explained by the fact that the increased concentration of the maleic anhydride increases the probability of maleic anhydride being present when the macroradicals

are being formed, thus decreasing the occurrence of β-scission. With the increase in the maleic anhydride concentration, the reaction of maleic anhydride with macroradicals likely occurs before the chain scission [87]. This observation was also explained as the suppressing of the degradation by the energy absorption of MA to melt as well as the cushion effect of the molten MA in the literature [88].

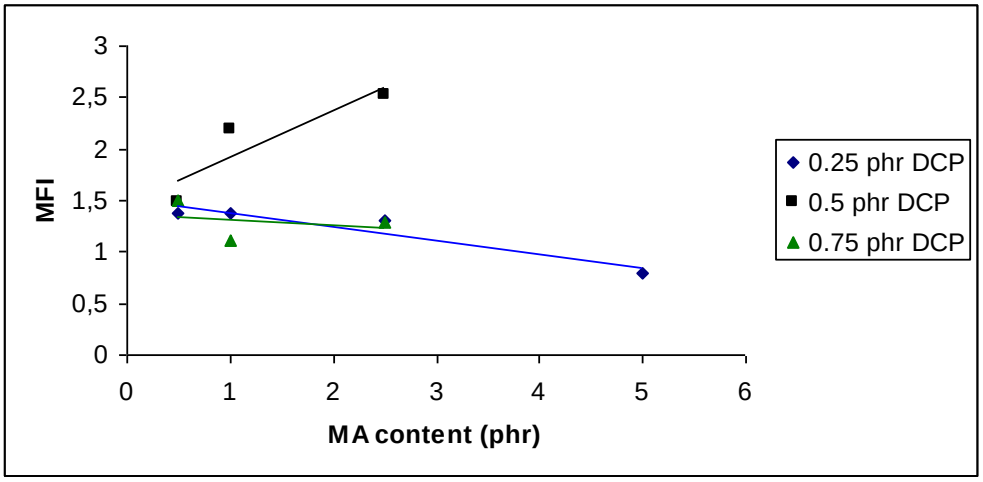

Figure 3.2 MFI values of MA-g-PP as a function of loading concentration of MA.

At 0.50 phr however, a remarkable increase was observed in MFI values as the loading concentration of MA increases. This could be explained by the occurrence of excess chain scission.

3.3 IR Spectroscopy

Attenuated Total Internal Reflection (ATR) Infrared Micro Spectroscopic Imaging system was used for the characterization of the samples. ATR spectrum of pure PP is given below in Figure 3.3. As seen, there is no carbonyl absorption peak and in addition, it is free from -OH observed around 3500cm^{-1}.

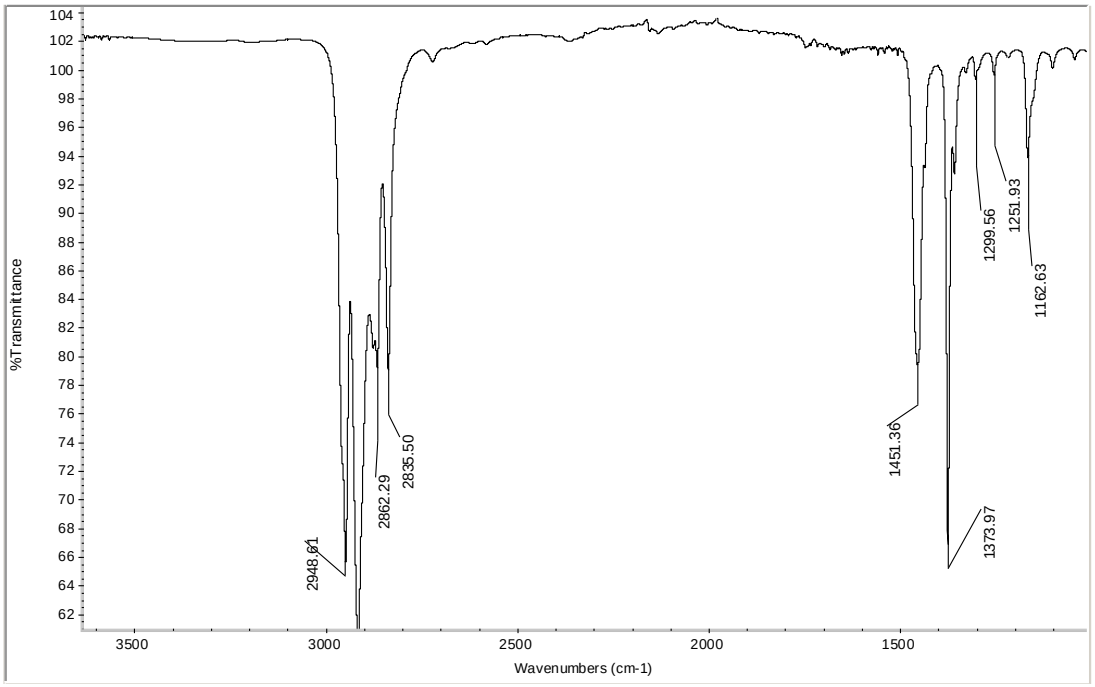

Figure 3.3 ATR spectrum of purified PP sample.

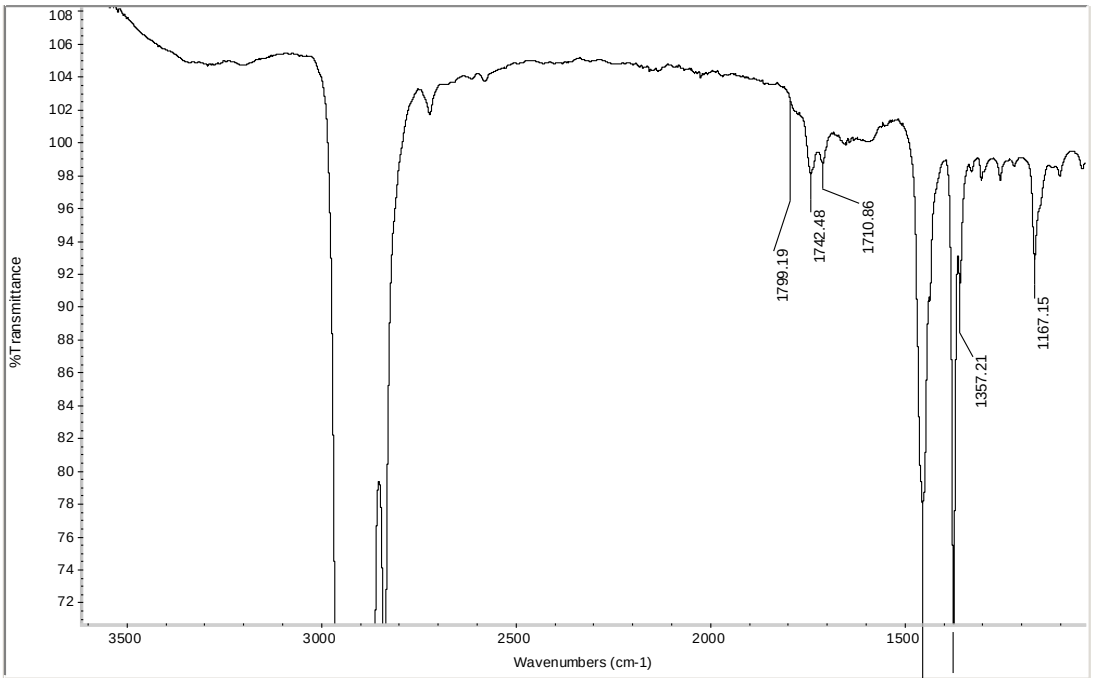

Figure 3.4 ATR spectrum of Ma-g-PP sample collected from Brabender.

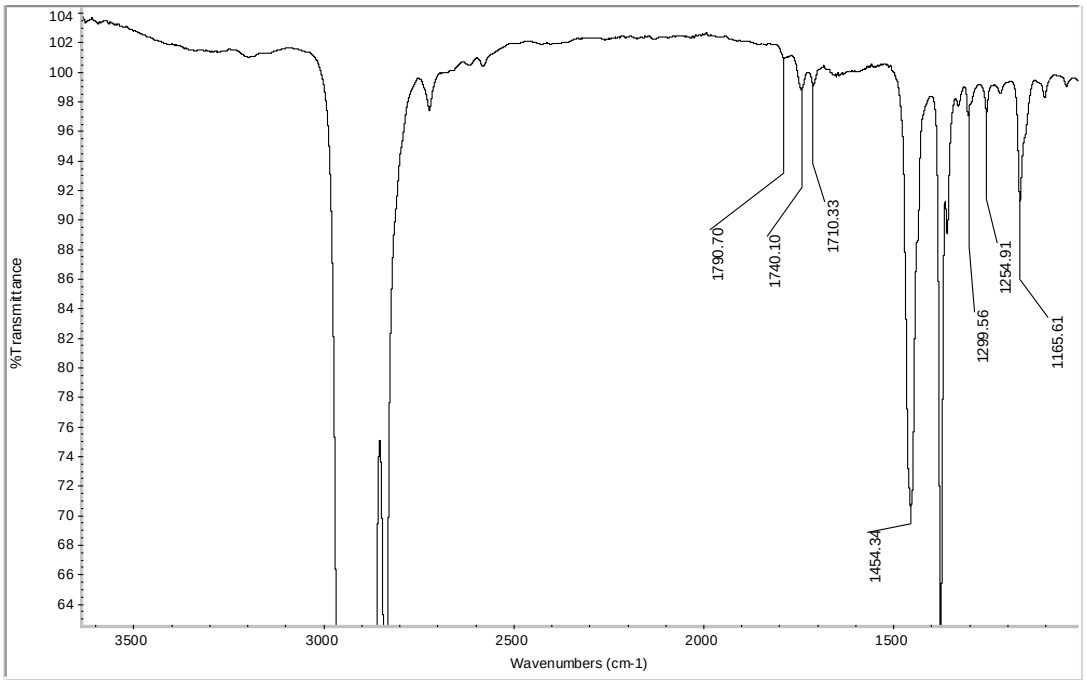

Figure 3.5 ATR spectrum of purified MA-g-PP samples.

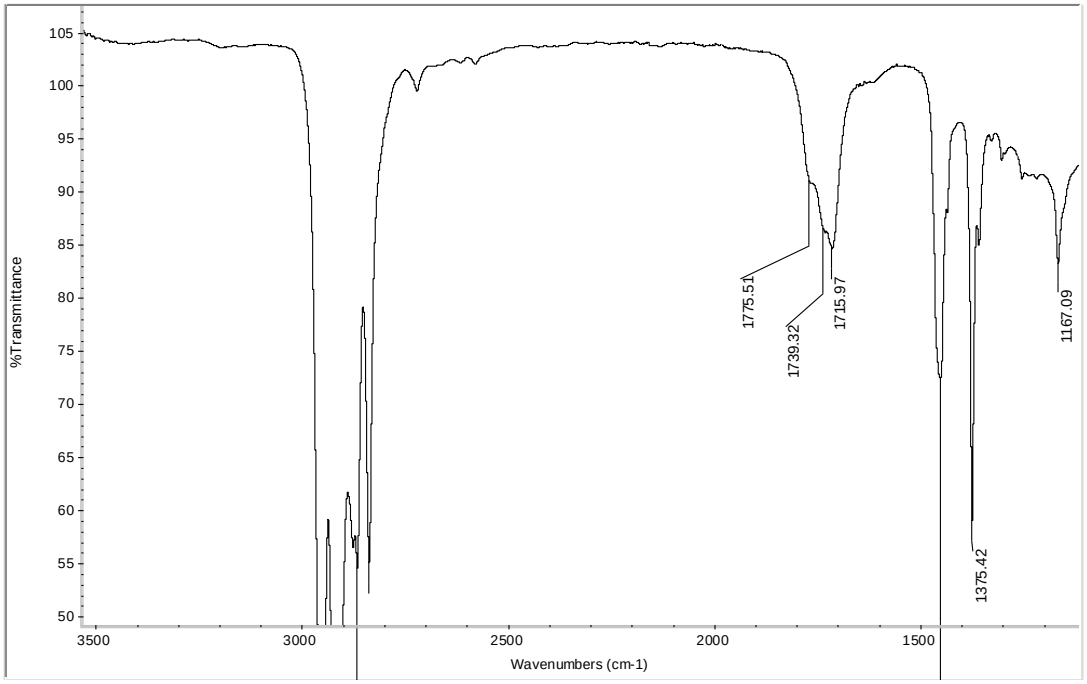

Figure 3.6 ATR spectrum of MA-g-PP samples subjected to the heat treatment after purification.

In the ATR spectra of all MA-g-PP samples given in Figure 3.4 - Figure 3.6 , unlike PP, there are characteristic peaks of the symmetric C=O stretching of anhydride groups in the region between 1720 - 1790 cm^{-1} which are consistent with the literature [17, 55, 59, 86, 89-95]. Vibrations at 1710 cm^{-1} and 1715 cm^{-1} due to the C=O stretching of the succinic acid form were observed at all spectra as well as at the spectrum of the sample subjected to the heat treatment. This can be explained by the ring opening reaction because of the moisture. Absorbance band observed between 3200- 3500 cm^{-1} also confirms the presence of -OH group. The absorbance band near 1740 cm^{-1} in Figure 3.4 and Figure 3.5 are attributed to carbonyl stretching in ester units [96] which could be formed as a result of the mono-esterification reaction of the pendant succinic anhydride groups with ethanol during the purification process. The ATR spectrum of MA-g-PP sample subjected to the heat treatment to provide complete cyclization of the acid groups to the anhydride form given in Figure 3.6 is free from OH absorption comparatively, and due to the dominant absorbance band at about 1775 cm^{-1}, it can be concluded that the main structure of MA-g-PP samples obtained consist of bridging type as well as an end grafting types of which possible structures are given in Figure 3.7.

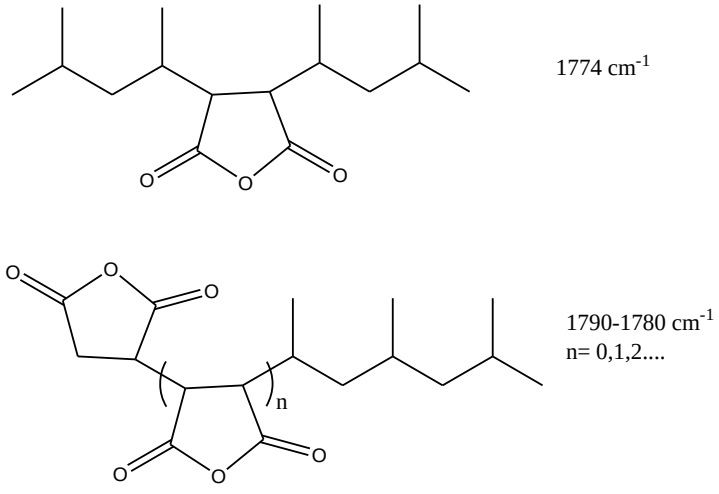

Figure 3.7 The suggested structures of the MA-g-PP samples and assignment of their characteristic IR absorption bands [85].

Literature indicates that the complete neutralization is confirmed by the disappearance of peaks in the range of 1700 – 1900 cm^{-1} and the appearance of peaks ranged from 1480 cm^{-1} to 1670 cm^{-1} in the FTIR spectra [17].

In this study, similar results are observed in the ATR spectra of the MA-g-PP samples neutralized with Na^{+}, Mg^{2+}, Ca^{2+} and K^{+} ions. New characteristic absorption bands, appeared near 1570 cm^{-1} in Figure 3.8, between 1560-1590 cm^{-1} in Figure 3.9, between 1535 cm^{-1}-1580 cm^{-1} in Figure 3.10, and at 1556 cm^{-1} in Figure 3.11 show the neutralized carboxylic groups in MA-g-PP with Na^{+}, Mg^{2+}, Ca^{2+} and K^{+} ions respectively.

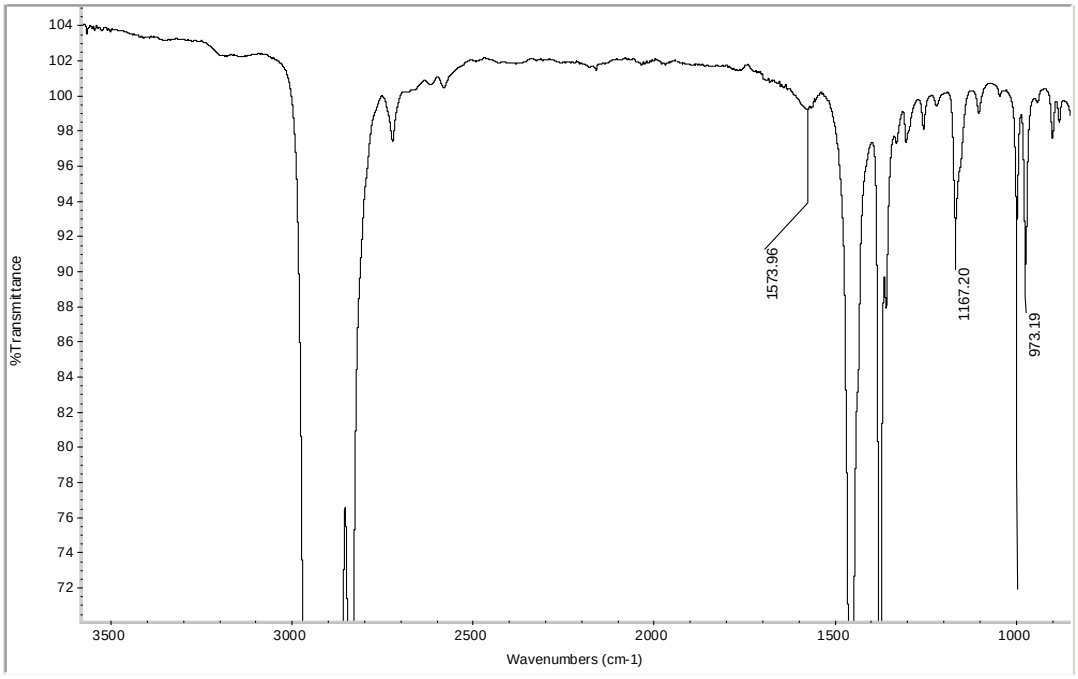

Figure 3.8 ATR spectrum of MA-g-PP sample neutralized with Na^{+} ion.

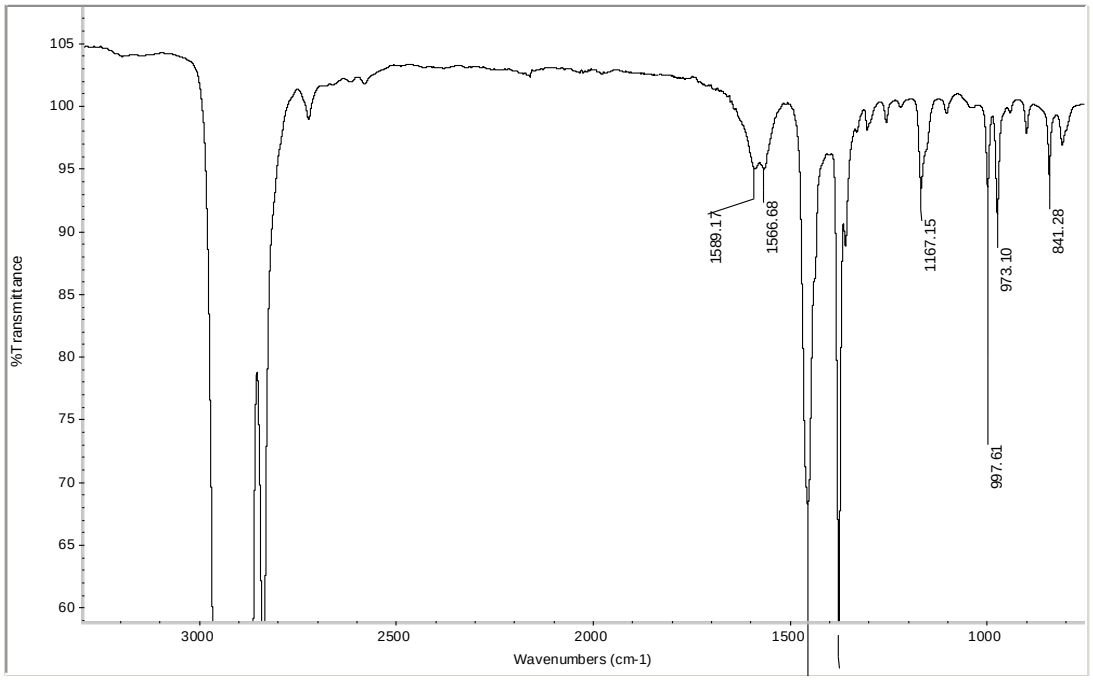

Figure 3.9 ATR spectrum of the MA-g-PP sample neutralized with Mg^{2+} ion.

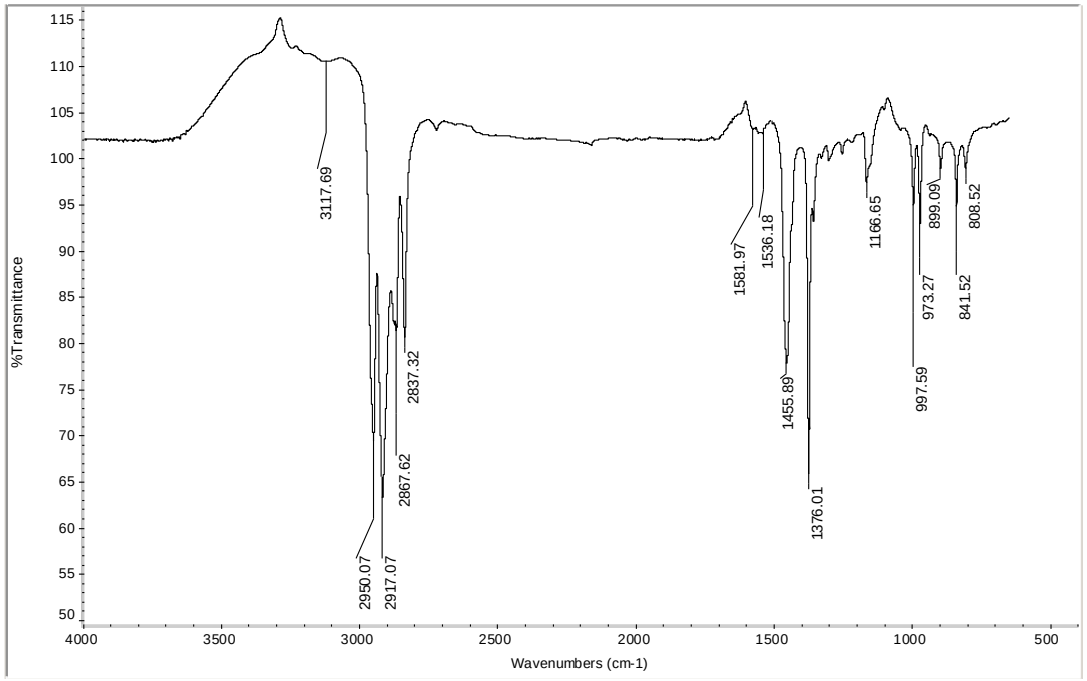

Figure 3.10 ATR spectrum of the MA-g-PP sample neutralized with Ca^{2+} ion.

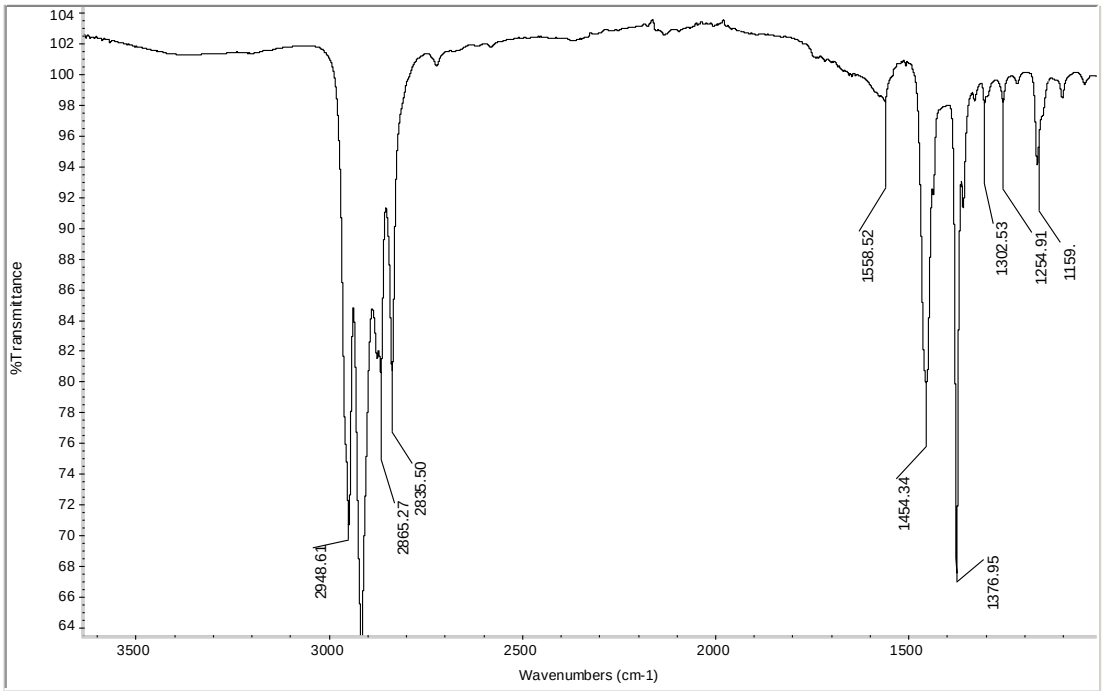

Figure 3.11 ATR spectrum of the MA-g-PP sample neutralized with K^+ ion.

3.4 Characterization of Crosslinked Resins

3.4.1 Swelling Index

The swelling index values of the resins obtained as a result of the procedures and calculations given in section 2.4.8.1 are summarized in Table 3.3.

Table 3.3 Swelling indexes of the resins

Samples	Swelling index	
	In xylene	In acetone
Na^+ neutralized MA-g-PP resin	108.1	*
K^+ neutralized MA-g-PP resin	114.6	*
Mg^{2+} neutralized MA-g-PP resin	121.8	*
Ca^{2+} neutralized MA-g-PP resin	130.5	*

*No swelling was observed.

For both monovalent and divalent atoms, it is seen that as the size of the ion increases, swelling index values increase as expected. The size effect of the ion can be explained as the space provided by ion within the polymer chains make the action of the solvent through the resin matrix easier and so increase swelling.

3.4.2 Gel Content

After the soxhlet extraction, the crosslinking degrees of the resins are calculated according to the equation given in section 2.4.8.2 and summarized in Table 3.4.

Table 3.4 The cross-linking degree of the resins.

Samples	Gel content (%)
Na^+ neutralized MA-g-PP resin	66.4
K^+ neutralized MA-g-PP resin	50.1
Mg^{2+} neutralized MA-g-PP resin	67.7
Ca^{2+} neutralized MA-g-PP resin	33.3

In crosslinking degree values, an inverse relationship with atomic size is observed in each valencies. As the size of the atom increases, the crosslinking degree of the resin decreases. It is expected and consistent with the trend in the swelling index values in a manner that as the crosslinking degree increases the extension of the polymer chain and the absorption of the solvent resulting in swelling will decrease.

3.5 Morphological Analysis

3.5.1 SEM

The SEM micrographs of the purified PP, purified MA-g-PP resin and MA-g-PP resins neutralized with Na^{+}, Ca^{2+}, Mg^{2+} and K^{+} ions are given in Figures 3.12 to 3.17.

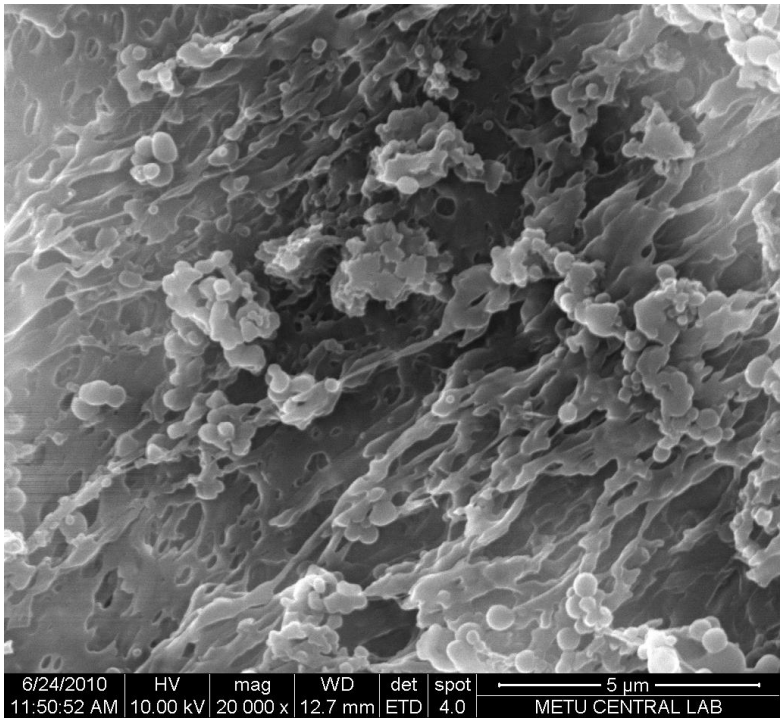

Figure 3.12 The SEM micrograph of purified PP.

In the purification process, precipitation of PP, which is dissolved in hot xylene, in non solvent result in formation of a foamy structure as a result of disentanglement and expansion of PP chains. Consequently purified PP has fibrous morphology as seen in Figure 3.12. Purified MA-g-PP sample in Figure 3.13 however, shows highly nodular morphology. This can be explained by the shrinkage of the MA-g-PP chains that had shorter length than PP chains as a result of chain scission occured in grafting, when they in contacted with non-solvent during the precipitation process. This

morphology is retained in MA-g-PP resins neutralized with Na^{+} (Figure 3.14), Ca^{2+} (Figure 3.15), Mg^{2+} (Figure 3.16) and K^{+} (Figure 3.17) ions.

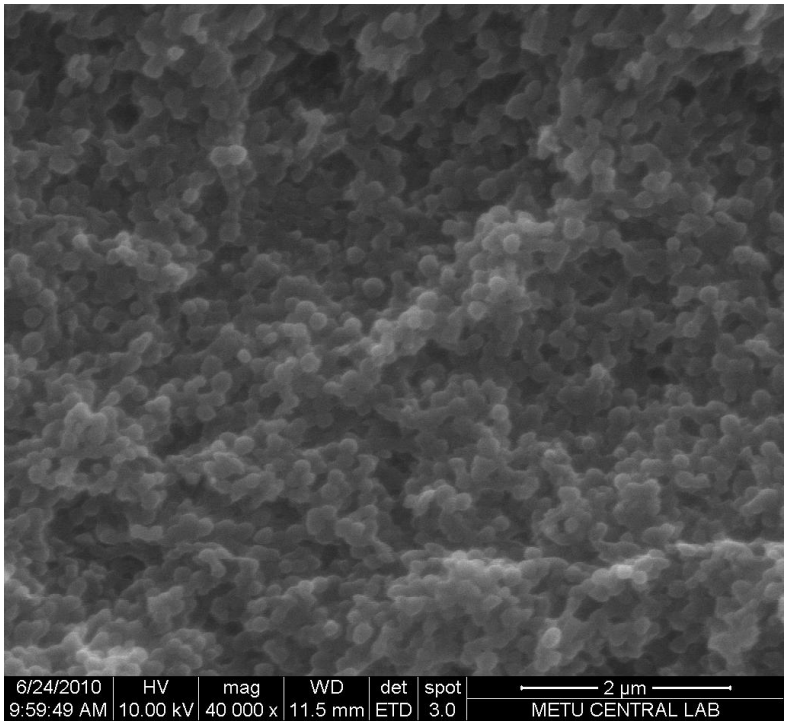

Figure 3.13 The SEM micrograph of purified MA-g-PP.

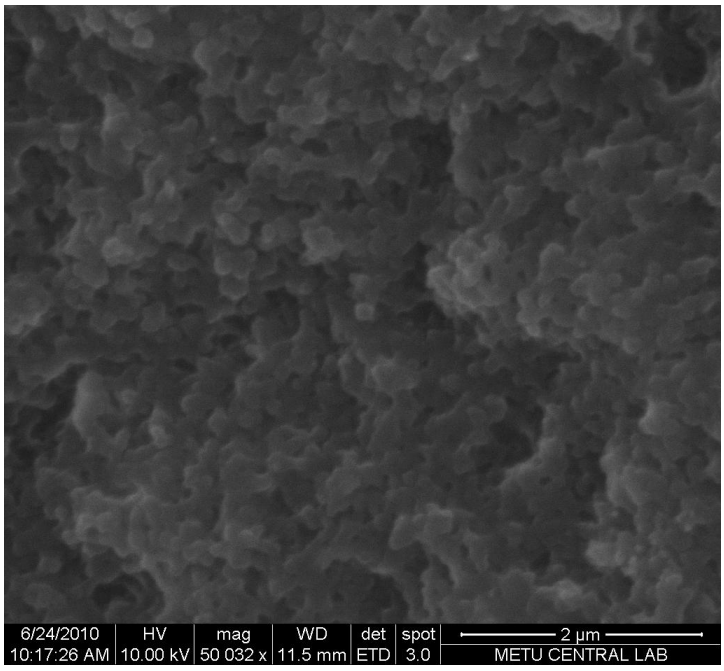

Figure 3.14 The SEM micrograph of Na^{+} neutralized MA-g-PP resin.

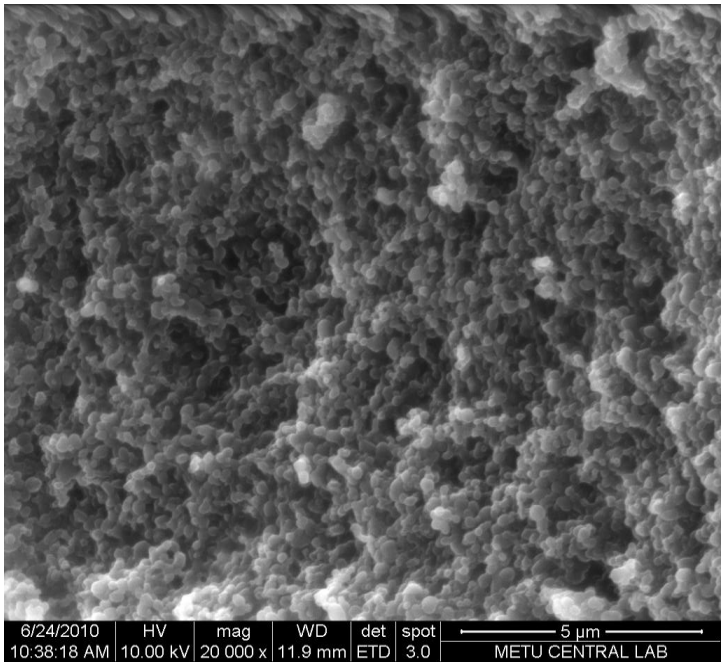

Figure 3.15 The SEM micrograph of Ca^{2+} neutralized MA-g-PP resin.

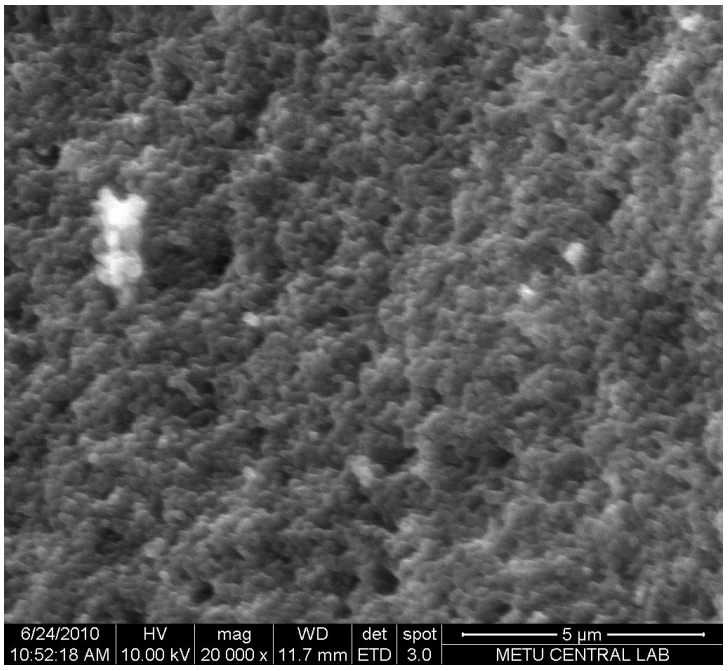

Figure 3.16 The SEM micrograph of Mg^{2+} neutralized MA-g-PP resin.

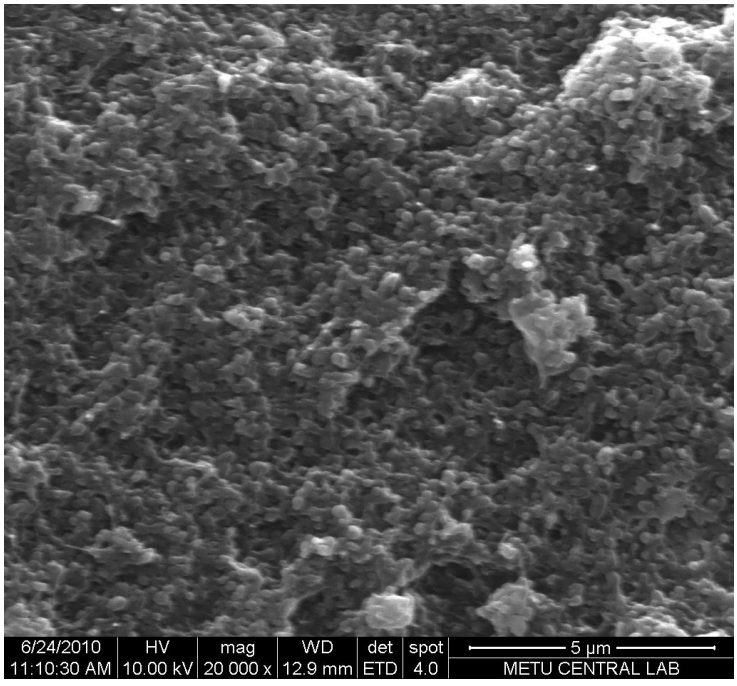

Figure 3.17 The SEM micrograph of K^{+} neutralized MA-g-PP resin.

3.5.2 SEM-EDX

The SEM-EDX analysis of the MA-g-PP resins neutralized by Na^{+}, Ca^{2+}, Mg^{2+} and K^{+} ions are given in Figures 3.18 to 3.21.

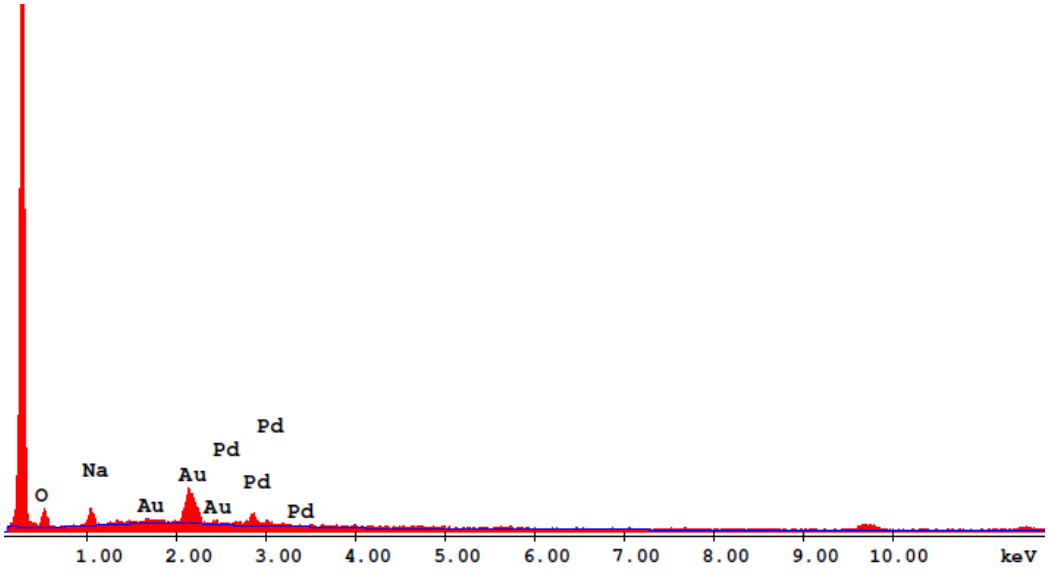

Figure 3.18 SEM-EDX element analysis of Na^{+} neutralized MA-g-PP resin.

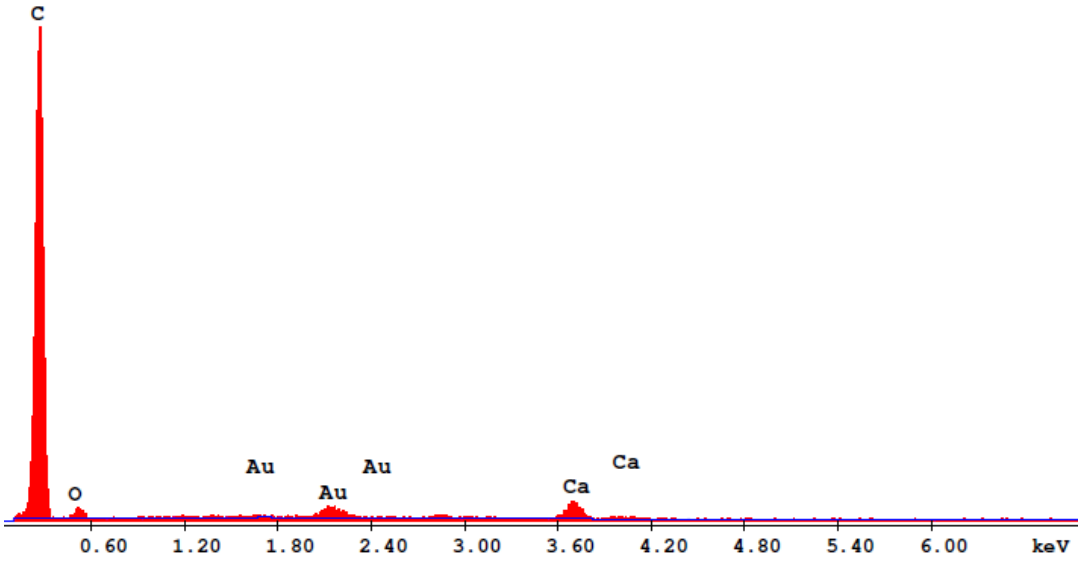

Figure 3.19 SEM-EDX Element analysis of Ca^{2+} neutralized MA-g-PP resin.

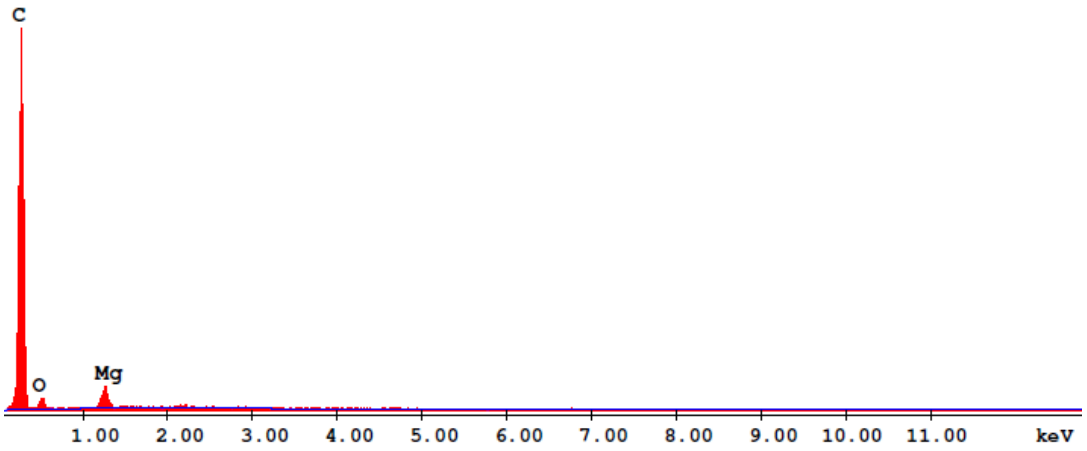

Figure 3.20 SEM-EDX Element analysis of Mg^{2+} neutralized MA-g-PP resin.

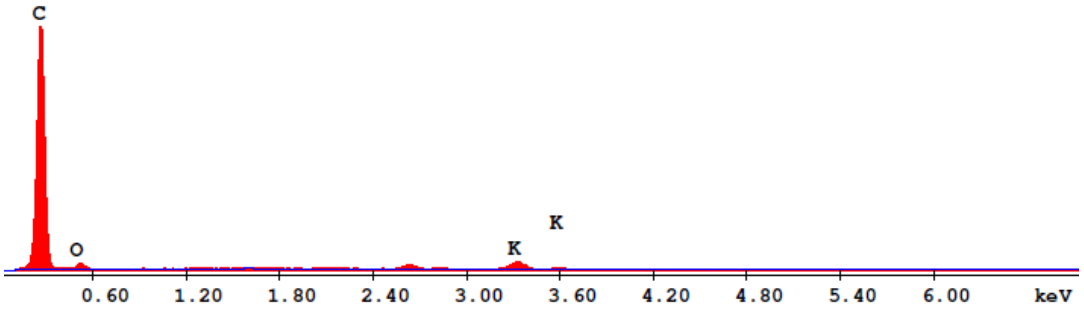

Figure 3.21 SEM-EDX Element analysis of K^{+} neutralized MA-g-PP resin.

SEM-EDX analysis results show the existence of the Na^{+}, Ca^{2+}, Mg^{2+} and K^{+} ions in MA-g-PP resins neutralized with these ions.

3.6 Characterization of Ion Exchange Properties

3.6.1 Ion Exchange Capacity

Total acid capacity of the non-neutralized MA-g-PP resin (H^+ form of resin) was found as 1.5 meq/g.

3.6.2 Metal Uptake at Different pHs

Sorption properties of non-neutralized MA-g-PP resin and the Ca^{2+}, Mg^{2+}, Na^+ and K^+ neutralized MA-g-PP resins towards $Cu^{2+,}$ Co^{2+}, Cd^{2+}, Pb^{2+} and Fe^{3+} ions at different pHs of 3, 4, 5 and 6 were determined in terms of the quantity of the metal ions uptaken per unit of dry weight of the resin (mg/g).

In uptake testing, if the resin has an affinity towards an ion and uptakes this ion, a decrease in the concentration of the solution of this ion in which the resin was incubated is expected after the removal of the resin from the solution.

However, at the end of uptake tests of Na^+, Mg^{2+} and K^+ neutralized and non-neutralized MA-g-PP resins for $Cu^{2+,}$ Co^{2+}, Cd^{2+}, Pb^{2+} ions at all pHs, it was seen that the absorbance values of the filtrate solutions after incubation are similar to that of initial solution in which resin is incubated. In other words, there was no change between the concentrations of the initial and filtrate solutions. So there were no succesful uptakes and it can be concluded that these resins have no affinity towards these ions. The data and measurements about the results of the uptake test of aforesaid resins for $Cu^{2+,}$ Co^{2+}, Cd^{2+}, Pb^{2+} ions are given Appendices A to E.

On the other hand, it was also found that except for Na^+ neutralized resin, all resins showed affinity to Fe^{3+} ion, and Ca^{2+} neutralized resin has affinity towards Cd^{2+} and

Pb^{2+} ions at specific pHs. Table 3.5 gives the general summary of the metal uptake testing results of MA-g-PP resins, and the detailed results of the uptake tests of the resins showing affinity to any ion are given in the following sections.

Table 3.5 Summary of the metal uptake results of MA-g-PP resins.

Metal ion uptake (mg/g)						
MA-g-PP resins	**pH**	**Co^{2+}**	**Pb^{2+}**	**Cu^{2+}**	**Cd^{2+}**	**Fe^{3+}**
Ca^{2+} neutralized	3	---	---	---	---	
	4	---	---	---	---	**8.66**
	5	---	**1.34**	---	---	
	6	---	**4.42**	---	**0.68**	
K^{+} neutralized	3	---	---	---	---	
	4	---	---	---	---	**3.93**
	5	---	---	---	---	
	6	---	---	---	---	
Na^{+} neutralized	3	---	---	---	---	
	4	---	---	---	---	---
	5	---	---	---	---	
	6	---	---	---	---	
Mg^{2+} neutralized	3	---	---	---	---	
	4	---	---	---	---	**0.86**
	5	---	---	---	---	
	6	---	---	---	---	
Non-neutralized (H-form)	3	---	---	---	---	
	4	---	---	---	---	**1.85**
	5	---	---	---	---	
	6	---	---	---	---	

--- no uptake

3.6.2.1 Pb^{2+} uptake of Ca^{2+} Neutralized MA-g-PP Resin

Absorbance values for Pb^{2+} ion standard solutions are shown in Table 3.6 and the related calibration curve is given in Figure 3.22.

Table 3.6 Absorbance values for Pb^{2+} ion standard solutions in Pb^{2+} uptake testing of Ca^{2+} neutralized MA-g-PP resin.

Concentration (ppm)	Absorbance
5	0.011
10	0.025
20	0.045
30	0.074
40	0.105
60	0.149
70	0.183

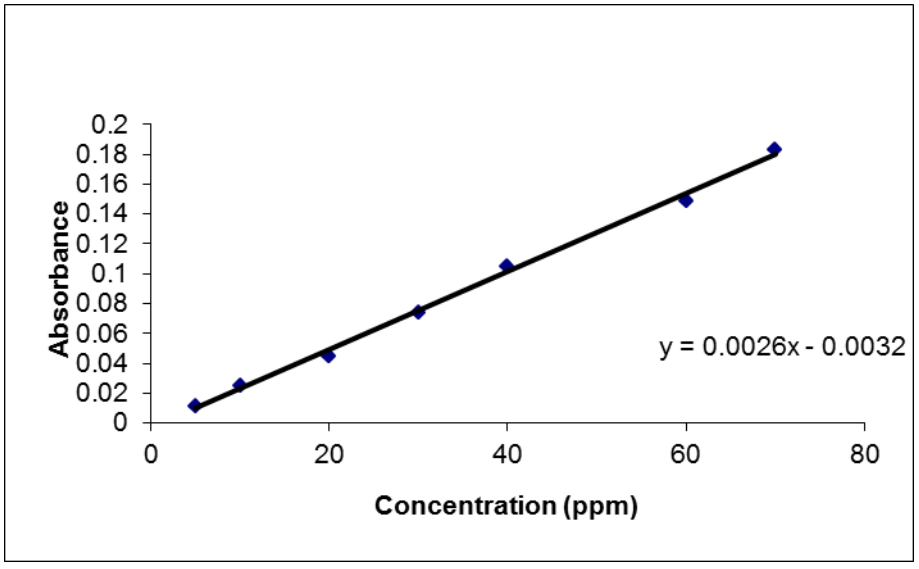

Figure 3.22 Calibration curve for Pb^{2+} ion in Pb^{2+} uptake testing of Ca^{2+} neutralized MA-g-PP resin.

Average absorbance values for Pb^{2+} of the filtrate solutions after the interaction with the Ca^{2+} neutralized MA-g-PP resin incubated in Pb^{2+} ion solution having a concentration of 20 ppm at different pHs are summarized in Table 3.7.

Table 3.7 Absorbance values for Pb^{2+} of the filtrate solutions in Pb^{2+} uptake testing of Ca^{2+} neutralized MA-g-PP resin after the incubation period.

Filtrate solution at pH	**Pb^{2+} absorbance**
3	0.043
4	0.047
5	0.014
6	*

*No absorbance

Values indicate that while the absorbance values of the filtrate solution at pH=3 and pH=4 are similar to that of 20 ppm standard solution, there is a remarkable decrease in the absorbance values of the filtrate solution at pH=5 and pH=6. This means that Pb^{2+} ions were uptaken by the resin at these pHs. Moreover, absorbance value at pH=6 was the same as background absorbance. So it was concluded that all Pb^{+2} ions in the solution having the concentration of 20 ppm were uptaken by the resin. To find out the maximum of the uptake capacity of Ca^{2+} neutralized resin towards Pb^{2+} ion, the resin was subjected to Pb^{2+} ion solution having a concentration of 60 ppm at pH=6. After the incubation time and filtration of the resin, absorbance value of the residual Pb^{2+} ions in the filtrate was measured as 0.034.

Corresponding concentrations uptaken by Ca^{2+} neutralized MA-g-PP resin and the Pb^{2+} ion uptake values of the resin are summarized in Table 3.8.

Table 3.8 Pb^{2+} ion concentrations uptaken by Ca^{2+} neutralized MA-g-PP resin and Pb^{2+} uptake values for Ca^{2+} neutralized MA-g-PP resin.

pH	Pb^{2+} ion concentration uptaken by resin	Pb^{2+} ion uptake of the resin (mg/g)
5	13.46 ppm	1.34
6	44.23 ppm	4.42

This can also be concluded that affinity of Ca^{2+} neutralized MA-g-PP resin towards Pb^{2+} ions increases by increasing pH of the medium.

3.6.2.2 Cd^{2+} Uptake of Ca^{2+} Neutralized MA-g-PP Resin

Absorbance values for Cd^{2+} ion standard solutions are shown in Table 3.9 and related calibration curve is given in Figure 3.23.

Table 3.9 Absorbance values for Cd^{2+} ion standard solutions in Cd^{2+} uptake testing of Ca^{2+} neutralized MA-g-PP resin.

Concentration (ppm)	Absorbance
1	0.163
2	0.298
2.5	0.377
5	0.684
10	1.072
20	1.938

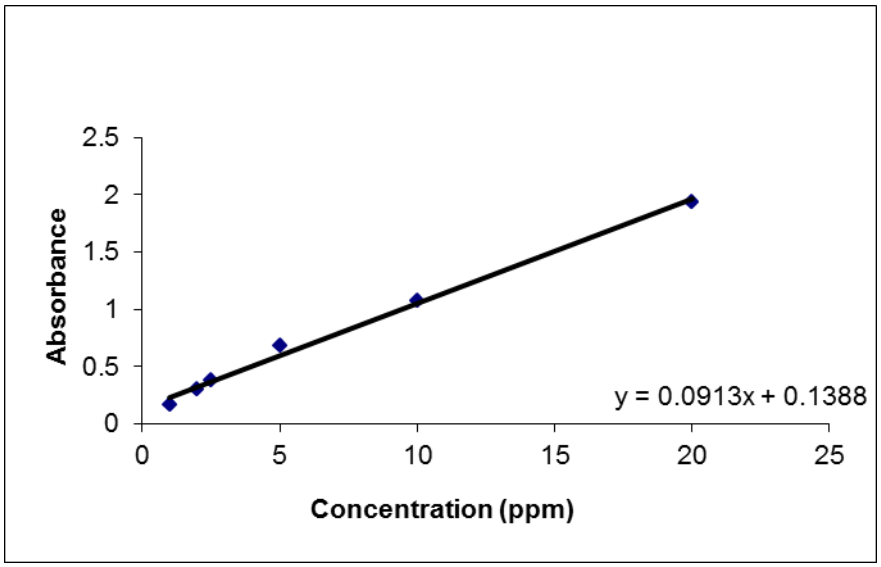

Figure 3.23 Calibration curve for Cd^{2+} ion in Cd^{+2} uptake testing of Ca^{2+} neutralized MA-g-PP resin.

Average absorbance values for Cd^{2+} of the filtrate solutions after the interaction with the Ca^{2+} neutralized resins at different pHs are summarized in Table 3.10.

Table 3.10 Absorbance values for Cd^{2+} of the filtrate solutions in Cd^{2+} uptake testing of Ca^{2+} neutralized MA-g-PP resin.

Filtrate solution at pH	**Cd^{2+} absorbance**
3	1.941
4	1.939
5	1.834
6	1.317

The absorbance values of the filtrate solution at pH=3, pH=4 and pH=5 are similar to that of 20 ppm standard solution again. However, there is a noteworthy decrease at pH=6 compared to the absorbance value of 20 ppm standard solution. This can be concluded that Cd^{2+} ions were uptaken by the resin especially at pH=6.

Corresponding concentration uptaken by Ca^{2+} neutralized MA-g-PP resin and and the Cd^{2+} ion uptake of the resin are given in Table 3.11.

Table 3.11 Cd^{2+} ion concentration uptaken by Ca^{2+} neutralized MA-g-PP resin and Cd^{2+} uptake value for Ca^{2+} neutralized MA-g-PP resin.

pH	Cd^{2+} ion concentration uptaken by resin	Cd^{2+} ion uptake of the resin (mg/g)
6	6.80 ppm	0.680

3.6.2.3 General evaluation of Fe^{3+} uptake

In characterizing the affinity of Ca^{2+}, Mg^{2+}, Na^{+}, K^{+} neutralized and non neutralized MA-g-PP resins towards Fe^{3+} ion at different pHs of 3, 4, 5 and 6, a different observation was seen. In the Fe^{3+} ion solutions, a red-brown color was observed when the stock solution of Fe^{3+} ion was added to acetate buffer solutions having the pHs of 3, 4, 5 and 6. It was also observed that as the pH of the buffer solution increased, red-brown color became denser. As the concentration of the conjugate base group in the buffer solution increases, formation of $Fe(OH)_3$ is favored.

$$A^- + H_2O \leftrightarrow HA + OH^- \quad (8)$$

$$Fe^{3+} + OH^- \rightarrow Fe(OH)_3 \quad (9)$$

This resulted in the breakdown of the pH adjustment and Fe^{3+} ion uptake testing of the resins actually was performed only at pH= 4.3. Absorbance values for Fe^{3+} ion standard solutions are shown in Table 3.12 and the related calibration curve is given in Figure 3.24.

Table 3.12 Absorbance values for Fe^{3+} ion standard solutions.

Concentration (ppm)	Absorbance
5	0.007
10	0.020
20	0.043
30	0.071
50	0.120
60	0.147
70	0.181

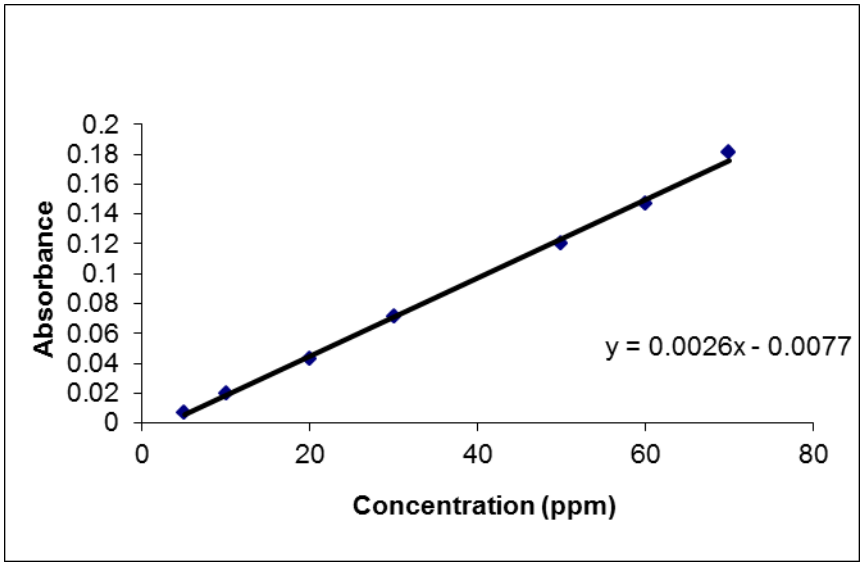

Figure 3.24 Calibration curve for Fe^{3+} ion.

Ca^{2+}, Mg^{2+}, Na^{+}, K^{+} neutralized and non neutralized MA-g-PP resins were firstly subjected to Fe^{3+} ion containing solution having a concentration of 20 ppm. For Ca^{2+}, K^{+} neutralized and non-neutralized MA-g-PP resins, similar absorbance values with background absorbance were obtained. So it was concluded that all Fe^{3+} ions in the solution having the concentration of 20 ppm were uptaken by these resins.

To find out maximum of the uptake capacity of Ca^{2+}, K^{+} neutralized and non-neutralized MA-g-PP resins, the resins were subjected to Fe^{3+} ion solution having a concentration of 60 ppm. For Ca^{2+} neutralized resins however, after getting similar absorbance value for filtrate solution with that of background absorbance again, resin was subjected to Fe^{3+} ion solution having a concentration of 90 ppm finally to find out maximum of the uptake capacity of Ca^{2+} neutralized MA-g-PP resins towards Fe^{3+} ion.

Average absorbance values for Fe^{3+} of the filtrate solutions after the interaction with Ca^{2+}, Mg^{2+}, Na^{+}, K^{+} neutralized and non-neutralized MA-g-PP resins are summarized in Table 3.13.

Table 3.13 Absorbance values for Fe^{3+} of the filtrate solutions in Fe^{3+} uptake testing of Ca^{2+}, Mg^{2+}, Na^{+}, K^{+} neutralized and non-neutralized MA-g-PP resins.

Resin	Absorbance
Na^{+} neutralized MA-g-PP resin incubated in 20 ppm Fe^{3+} ion solution	0.042
Mg^{2+} neutralized MA-g-PP resin incubated in 20 ppm Fe^{3+} ion solution	0.021
Non-neutralized MA-g-PP resin incubated in 60 ppm Fe^{3+} ion solution	0.100
K^{+} neutralized MA-g-PP resin incubated in 60 ppm Fe^{3+} ion solution	0.044
Ca^{2+} neutralized MA-g-PP resin incubated in 90 ppm Fe^{3+} ion solution	0.005

Corresponding Fe^{3+} ion concentrations uptaken by MA-g-PP resins and the Fe^{3+} ion uptakes of the resins are summarized in Table 3.14.

Table 3.14 Fe^{3+} ion concentrations uptaken by resins and Fe^{3+} uptake values for resins.

MA-g-PP Resins	Fe^{3+} ion concentration uptaken by resin	Fe^{3+} ion uptake of the resin (mg/g)
Mg^{2+} neutralized	8.62 ppm	0.86
Non-neutralized	18.50 ppm	1.85
K^{+} neutralized	39.30 ppm	3.93
Ca^{2+} neutralized	86.6 ppm	8.66

Conclusively, Ca^{2+} neutralized MA-g-PP resin has highest affinity for Fe^{3+} uptake, almost 10 times of Mg^{2+} neutralized MA-g-PP resin and 5 times of non-neutralized MA-g-PP resin.

3.6.3 Evaluation of the Concentration Effect on Metal Uptake

Absorbance values for Pb^{2+} ion standard solutions in concentration effect test are shown in Table 3.15 and the related calibration curve is given in Figure 3.25.

Table 3.15 Absorbance values for Pb^{2+} ion standard solutions

Concentration (ppm)	Absorbance
10	0.009
30	0.026
40	0.034
60	0.049
70	0.057

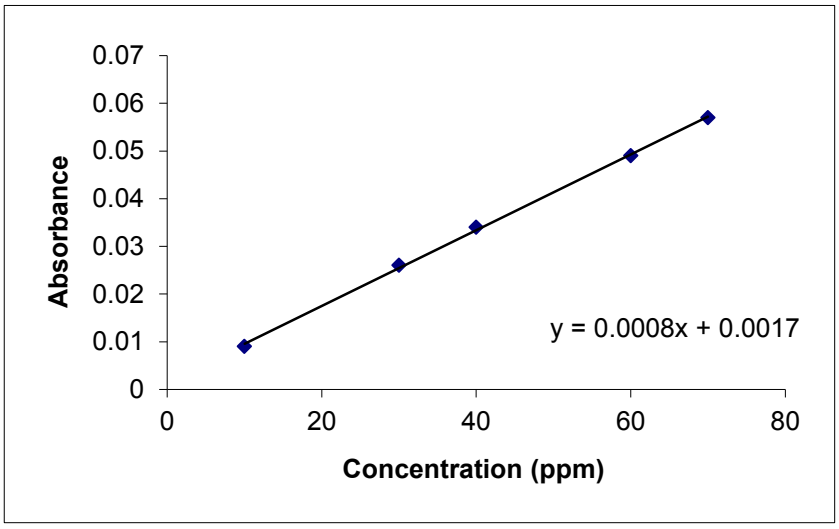

Figure 3.25 Calibration curve for Pb^{2+} ion in concentration effect test.

Average absorbance values for Pb^{2+} of the filtrate solutions after the interaction with the Ca^{2+} neutralized resins and corresponding Pb^{2+} ion uptake of the resins are summarized in Table 3.16. and Table 3.17. respectively.

Table 3.16 Absorbance values for Pb^{2+} of the filtrate solutions in concentration effect test.

Ca^{2+} neutralized MA-g-PP resin incubated in a solution of Pb^{2+} ion having a concentration of	**Pb^{2+} absorbance for filtrate solution**
40 ppm	0.023
60 ppm	0.032
70 ppm	0.041

Table 3.17 Pb^{2+} uptake values for Ca^{2+} neutralized MA-g-PP resins

Ca^{2+} neutralized MA-g-PP resin incubated in	**Pb^{2+} ion uptake of the resin (mg/g)**
40 ppm	4.21
60 ppm	3.75
70 ppm	3.13

It is seen that as the Pb^{2+}concentration of the solution in which the resin is incubated increases, uptake of the resin decreased. This could be explained by the distribution effect formed by Pb^{2+} ions in the medium. As the amount of Pb^{2+} ions in the medium increases, the mobility of these ions in the solution and through the resin matrix becomes difficult, and as a result interchange of Ca^{2+} ions in the resin with the Pb^{2+} ions in the solution is low.

3.6.4 Evaluation of Rate of Metal Uptake

The rate of uptake for Cd^{2+} and Pb^{2+} ions by Ca^{2+} neutralized resin is calculated as follows. It is assumed that at 20ºC and at pH=6, the state of equilibrium is established within 10 h. The rate of metal uptake is expressed as the percentage of the attainment at the state of equilibrium in Table 3.18. If "X" mg of metal ions were uptaken after 1 h and "Y" mg of metal ions were uptaken at equilibrium, i.e., the measure of percentage of equilibrium attained after 1 hour then would be expressed as; (X/Y)x100 [78].

Table 3.18 Rates of metal ion uptake for Ca^{2+} neutralized MA-g-PP resin

Time (h)	**Pb^{2+}**	**Cd^{2+}**
0.5	20.4	25.6
1.5	60.2	55.3
2.5	93.2	98.3
3.5	100.0	100
4.5	---	---
5.5	----	---

Table 3.18 showed that the uptake of both Cd^{2+} and Pb^{2+} ions by the resin completed within approximately three hours.

3.6.5 Regeneration

In order to make an evaluation about the possibility and the extent of reuse of Ca^{2+} neutralized MA-g-PP resin, after the ion uptake tests, the resins that showed affinity to Pb^{2+} and Cd^{2+} ions were subjected to concentrated acid solution. After the filtration of the solid part, the remaining solutions were investigated by AAS for the release of the metal ions. Table 3.19 shows the percent regeneration of these resins.

Table 3.19 The percent regeneration of the resins.

Resin	**Cd^{2+}**	**Pb^{2+}**
Ca^{2+} neutratized MA-g-PP	69.3	75.3

CHAPTER 4

CONCLUSIONS

In the first part of this thesis, we dealt with the melt grafting MA onto PP by using DCP as an initiator. It was examined whether the DCP and MA concentration introduced to the grafting medium had an effect on the MA degree of the MA-g-PP samples. It was seen that both of the MA and DCP concentration introduced had no distinguishable effect on the MA degree of the MA-g-PP samples. It was also shown that the synthesized MA-g-PP samples had low molecular weight due to the chain scission or degradation that occurred simultaneously with grafting. Grafting of anhydride group on PP was characterized by ATR.

In the following part, MA-g-PP was neutralized with K^+, Na^+, Mg^{2+} and Ca^{2+} ions and peroxide crosslinking of these samples was performed. Characterization of the ionic sites of the resins was carried out by SEM-EDX analysis and ATR again. SEM of the resin were also taken.

In the last part of the work, ion exchange properties of the resins were investigated. At this scope, sorption properties of the MA-g-PP samples neutralized with K^+, Na^+, Mg^{2+} and Ca^{2+} ions and non-neutralized MA-g-PP resin towards Cu^{2+}, Co^{2+}, Cd^{2+}, Pb^{2+} and Fe^{3+} ions at different pHs of 3, 4, 5 and 6 were studied.

It was seen that, except for the Na^{+} neutralized resin, all resins showed affinity to Fe^{3+} ion due the high charge of the Fe ion. Since, generally it is found and accepted that as the charge of the ion increases, the selectivity of a resin to this ion increases. However, in this study it is also observed that at high pHs (> 4.3) interchanging of Fe^{+3} ions with the ions on the resin is limited or blocked by the formation of $Fe(OH)_3$.

It was also seen that while K^{+}, Na^{+} and Mg^{2+} neutralized MA-g-PP resins didn't show any affinity towards Cu^{2+}, Co^{2+}, Cd^{2+} and Pb^{2+} ions, Ca^{2+} neutralized resin however, showed affinity towards Cd^{2+} and Pb^{2+} ions at certain conditions.

For Ca^{2+} neutralized resin, it was observed that at low pHs or acidic medium resin showed no affinity towards any of the metal ions. This is mostly due to the weakly acidic character of carboxyl group or neutralized carboxyl group of the resin. In acidic medium, neutralized functional parts of the resins prefer hydrolyzing instead of exchanging counter ions with the ions in the solution. It was also seen that at higher pHs, it showed affinity towards ions which is an expected character for weakly acidic resins. At pH=5 and pH=6, the affinity of the resin increases little for the Cd^{2+} and mostly Pb^{2+} ions. However, it shows no affinity to the Cu^{2+} and Co^{2+} ions. So, the results showed that MA-g-PP resins have more affinity to Cd^{2+} and Pb^{2+} ions than Ca^{2+} ion which result with the interchanging of these ions. In addition to this, it was also concluded that resin has more affinity to Ca^{2+} ion than Cu^{2+}, and Co^{2+} ions.
This can be explained by the size of the ions. As the size of the ion increases, sorption of this ion by the resin or extent of the exchange will increase. Since the atomic size of Ca^{2+} ion is larger than both Cu^{2+} and Co^{2+} ions, resin preferably shows affinity to hold Ca^{2+} ion instead of exchanging it with Cu^{2+} or Co^{2+} ions in the solution. In the presence of larger atomic sized Cd^{2+} and Pb^{2+} ions however, it will be easier for the resin to exchange Ca^{2+} ion with these two ions.

For K^+, Na^+ and Mg^{2+} neutralized MA-g-PP resins, at high pHs (especially at pH=6), although showing affinity to Cu^{2+}, Co^{2+}, Cd^{2+} and Pb^{2+} ions was expected due to the ionic size effect mentioned above, it was seen that these resins have higher affinity to hydrolyze to form carboxylic acid at all pHs.

In addition to all, as general, limited or lack of affinity of the resins may also be due to the low number of accessible functional groups in the resin and low capacity of the resins. Since grafting degree of MA on the PP was limited as a consequence of grafting nature, the number of introduced carboxylic groups on resin was low.

REFERENCES

[1] F. Helfferic, *Ion Exchange*, (1962).

[2] A. A. Zagorodni, *Ion Exchange Materials*, (2007).

[3] C.E. Harland, *Ion Exchange Theory and Practice*, (1994).

[4] K. Dofrfner, *Ion Exchangers Properties and Applications*, (1972).

[5] J.E. Salmon, D. K. Hale, *Ion Exchange a Laboratory Manual*, (1959).

[6] D. Tripathi, *Practical Guide to Polypropylene*, Rapra Technology Limited, (2002).

[7] H. P. Frank, *Polypropylene*, Gordon and Breach Science Publishers, N. Y.,(1968).

[8] A.M.M. Baker, J. Mead, "*Thermoplastics," Handbook of Plastics, elastomers and composites*, C.A. Harper, ed., McGraw-Hill Professional, (2004).

[9] R. Ebewele, *Polymer Science and Technology*, CRC Press, (2000).

[10] R.A. Petrick, *Polymer Structure Characterization* (From Nano to Macro Organization), The Royal Society of Chemistry, (2007).

[11] H.S. Hamid, M. B. Amin, A.G. Maadhah, *Handbook of Polymer Degradation*, Marcel Dekker Inc., (1992).

[12] P.E. Moore Jr., *Polypropylene Handbook*, Hanser Publishers, Munich-New York, (1996).

[13] E.C. Carraher, *Polymer Chemistry*, Mercel Dekker, Inc., (2003).

[14] H.G. Karian, *Handbook of Polypropylene and Polyropylene composites*, Marcel Dekker Inc., (2003).

[15] Y. Bondar, H.J. Kim, H.S. Yoon, *Reactive and Functional Polymers*, 58, (2004), 43.

[16] S.L. Woo, Y. Bondar, H.D. Han, *Radiation Physics and Chemistry*, 15,(2007), 342

[17] H. Yu, J. He, *Polymer*, 41, (2000), 891.

[18] H.J. Park, C. Na, *Journal of Colloid and Interface Science* 46, (2006), 301.

[19] S.E. Artemenko, T. P. Ustinova, *Fibre Chemistry*, 35, (2003), 1.

[20] Y. Minoura, M. Ueda, S. Mizunuma, M. Oba, *J. Appl. Polym. Sci*.,13, (1996),1625.

[21] G. Ruggeri, M. Aglietto, A. Petragnani, F. Ciardelli, *Eur. Polym. J*, 19, (1983),863.

[22] S.H. Choi, Y.C. Nho, G.T. Kim, *J. Appl. Polym. Sci.,* 71, (1999), 643.

[23] K.P. Lee, H.J. Kang, D.L. Joo, *Radiat. Phys. Chem*., 60, (2001), 473.

[24] M. Kim, K. Saito, S. Furusaki, *J. Membr. Sci*., 85, (1993), 21.

[25] S.H. Choi, Y.C. Nho, *Anal. Sci. Technol.* 12, (1997), 7.

[26] S.H. Choi, Y.C. Nho, *J. Appl. Polym. Sci.,* 71, (1999), 999.

[27] M. Kim, K. Saito, *React. Funct. Polym.,* 40, (1999), 275.

[28] M. Kim, K. Saito, S. Furusaki, *J. Chromatogr.*, A585, (1991), 45.

[29] J. Wei, K. Zhao, Z. Jian, H. Zhang, *MACE*, (2010), 1870

[30] B. Gupta, V. Kanda, P. Sethi, S.Saxena, *Indian J. of Fibre and Textile Research*, 33, (2008), 431.]

[31] H.J. Park, C.K. Na, j. Colloid Interface Sci, 1,(2006), 301.

[32] B. Bae, D. Kim, *J. Membrane Sci*. 220, (2003), 75.

[33] X. Tan, Y. Xu, *Radiation Effects & Defects in Solids*, 163, (2008), 107.

[34] T.I.S. Ngah, M.M. Nasef , H. Saidi, K.Z.M. Dahlanc, J. of Aplp.Polym. Sci., 77 (1999), 1877.

[35] R.M. Ho, A. C. Su, C.H. Wu, S.L. Chen, *Polymer*, 34, (1993), 3264.

[36] N.G. Gaylord, M.K. Mishra , *J. Polym. Sci. Polym. Lett. Ed*., 21, (1983), 23.

[37] Y.J. Sun, G.H. Hu, M. Lambla, *J. Appl. Polym. Sci*., 57, (1995), 1043.

[38] R. Rengarajan, M. Vicic, S. Lee, *Polymer*, 30, (1989), 933.

[39] R. Rengarajan, M. Vicic, S. Lee, *J. Appl. Polym. Sci.,* 39, (1990), 1783.

[40] S. Lee, R. Rengarajan, V.R. Parameswaran, *J. Appl. Polym. Sci*., 41, (1990), 1891.

[41] F. Mitsuyoshi, M. Kondou, *J. App. Poly. Sci.*, 85, (2003), 762.

[42] M. Kim, K. Saito, *Reactive and Func. Poly.*, 40, (1999), 275.

[43] C. Eun-Young, H. Strathmann, J. Park, *J. Membrane Sci.,* 268, (2000), 165.

[44] R. Zhang, Y. Zhu, J. Zhang, W. Jiang, J. Yin, *J. of Poly. Sci.: Part A: Poly. Chem.*, 43, (2005), 5529.

[45] Y. Minoura, M. Ueda, S. Mizunuma, M. Oba. *J Appl Polym Sci*., 13, (1996), 1625.

[46] G. Ruggeri, M. Aglietto, A. Petragnani, F. Ciardelli, *Eur Polym J*, 19, (1983), 863.

[47] N.G. Gaylord, M. Mehta, *J. Polym. Sci. Polym. Lett. Ed*.,20, (1982), 481.

[48] Gaylord N.G, Mishra MK. *J Polym Sci Polym Lett Ed*, 21, (1983), 23.

[49] A.S. Bratawidjaja, I. Gitopadmoyo, Y. Watanabe, T. Hatakeyema, *J. of Appl. Polym. Sci.*, 34, (1984), 1141.

[50] R. Rengarajan, V. R. Parameswaran, S. Lee, M. Vicic, P.L. Rinaldi, *Polymer*, 31, (1990), 1703.

[51] Singh RP. *Prog Polym Sci*,17,251,(1992)Paul JR. In: Paul DR, Newman S, editors. Polymer Blends. New York:

[52] C. Kelly, L. Sunggyu, *Polym. Eng. Sci*., 44, (2004), 1636.

[53] Academic Press, 1978 (Chap. 12)

[54] N. G. Gaylord, *Chemtech;* 19,(1989), 435.

[55] B.D. Roover, M. Sclavons, V. Carlier, J. Devaux, R. Legras, A. Momtag, J. *Polym. Sci. Part A: Polym Chem*, 33, (1995), 829.

[56] W. Heinen, C.H. Resenmoller, C.R. Wenzel, H.J.M. de Gront, J. Lurtenburg, M. van Duin, *Macromolecules*, 29, (1996), 1151.

[57] K.E. Russell, E.C. Kelusky, *J. Polym. Sci. Polym. Chem. Ed*., 26, 2273,(1988)

[58] S. Dean, Y. Jinghui, Y.Zhanhai, W. Yong, *Polymer*, 42, (2001), 5549.

[59] M. Sclavons, V. Carlier, B.D. Roover, P. Franquinet, J. Devaux, R. Legras, J. *Appl. Polym. Sci*., 62, (1996), 1205.

[60] E. Borsig, A. Fieflerova, M. Lazar, *J. Macromol. Sci-Chem*., A16, (1981), 513.

[61] I. Chodak, M. Lazar, *Angew Makromol Chem*, 106, (1982), 153.

[62] I. Chodak, M. Lazar, *J. Appl. Polym. Sci.*, 32, (1986), 5431.

[63] E. Borsig, A. Fieldlerova, L. Rychla, M. Lazar, *J Appl Polym Sci*., 37, (1989), 467.

[64] I. Chodak, E.Zimanyova, *Eur. Polym. J*.,20, (1984), 81.

[65] B. K. Kim, K.J. Kim, *Adv. Polym. Techn.*, 12, (1993), 263

[66] P. Hudec, L. Obdrzalek, *Angew. Makromol. Chem.*,89, (1980) 41.

[67] M. Dorn, *Adv. Polym. Technol*.,5, (1985), 87.

[68] C. Tzoganakis, J. Vlachopoulos, A.E. Hamielec, *Polym. Eng. Sci*., 28, (1988), 170.

[69] W.L. Hawkins, *Degradation and Stabilization of Polymers* New York, Applied Science, (1975).

[70] Q. Yu , S. Zhu, *Polymer*, 40, (1999), 2961.

[71] A.V. Shenoy, D.R. Saini, *Thermoplastic Melt Rheology and Processing*, Marcel Dekker, Inc., Newyork, (1996).

[72] T.Bremner, A.Rudin, *J. Appl. Polym. Sci.*, 41, (1990), 1617.

[73] A. Singh, V. Parmar, *Int. J. Polym. Mat.*, 57, (2008), 1019.

[74] M.V. Tarase, A.B. Zade, B.V. Gurnule, 108, (2008), 738.

[75] M.M. Jadhao, L.J. Paliwal, N.S. Bhave, Journal of Applied. Polymer Science, 109, (2008), 508.

[76] A.W. Trochimczuk, *Eur. Polym. J.* 34, (1998), 1654.

[77] Y. Bondar, H.J. Kim, S.H. Yoon, Y.J. Lim, *Reac. and Func. Polym.*, 58, (2004), 43.

[78] J.D. Joshi, N.B. Patel, S.D. Patel, *J. of Macromol. Sci., Part A: Pure and App. Chem.*, 43, (2006), 1167.

[79] A.W. Trochimczuk, B.N. Kolarz, D.J. Bartkowiak, *Eur. Polym. J.*, 37, (2001), 559.

[80] W. Qiu, T. Endo, T. Hirotsu, *J. Appl. Polym. Sci.*, 102, (2006), 3830.

[81] Z. Farao, E.Takashi, Q.Wulin, *J.. Appl. Poly. Sci*, 84, (2002), 1971.

[82] N.Chaoren, S. Stitisayidah, K. Azizon, *Polym. Test*., 25, (2006), 413.

[83] S.H.P. Bettini, J.A.M. Agnelli, *J. Appl. Polym. Sci*., 74 (1999), 247.

[84] H.İ. Halimatuddahliana, H. Md. Akil, *Int. J. Polym. Mat.,* 54, (2005), 1169.

[85] H. J. Park, C.K. Na, *J. Colloid and Interface Sci*., 301, (2006), 46.

[86] A.R. Oromehie, S.A.Hashemi, I.G. Meldrum, D.N. Waters, *Polym. Int.,* 42, (1997), 117.

[87] S.H.P. Bettini, J.A.M. Agnelli, *J. App. Polym. Sci*., 85, (2002), 2706.

[88] W. Qui, T. Endo, T.Hirotsu, *Eur. Polym. J.*, 41, (2005), 1979

[89] G.C. Chitanu, I. Popescu, A. Caprov, *Revue Roumaine de Chimie*, 51, (2006), 923.

[90] M. Sclavons, M. Laurent, J. Devaux, V. Carlier, *Polym.*, 46, (2005), 8062.

[91] Q. Wang, C. Liu, Z. Chen, Polymer, 33, (2001), 522.

[92] F. Zhang, T. Endo, W. Qui, L. Yang, T. Hirotsu, *J. Appl. Polym. Sci*., 84, (2002), 1971.

[93] M. Sclavons, P. Franquinet, V. Carlier, G. Verfailie, I. Fallais, R. Legras, M. Laurent, F.C. Thyrion, *Polym*., 41, (2000), 1989.

[94] K.Y. Kim, S.C. Kim, *Macromol. Symp*., 214, (2004), 289.

[95] W. Qiu, T. Endo, T. Hirotsu, *Eur. Polym. J*., 41, (2005), 1979.

[96] E.L. Saier, L. Petrakis, L.R. Cousins, W.J. Heilman, JF. Itzel, *J. Appl. Polym. Sci., 12*, (1968), 2191.

APPENDIX A

UPTAKE TEST RESULTS OF Ca^{2+} NEUTRALIZED MA-g-PP RESIN

Table A.1 Absorbance values for Co^{2+} ion standard solutions in Co^{2+} uptake testing of Ca^{2+} neutralized MA-g-PP resin.

Concentration (ppm)	Absorbance
2	0.059
5	0.147
10	0.271
20	0.462
30	0.661

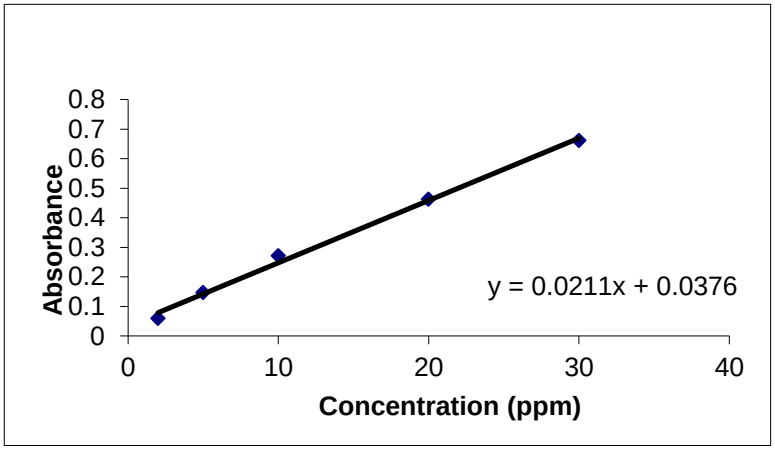

Figure A.1 Calibration curve for Co^{2+} ion in Co^{2+} uptake testing of Ca^{2+} neutralized MA-g-PP resin.

Table A.2 Absorbance values for Co^{2+} of the filtrate solutions in Co^{2+} uptake testing of Ca^{2+} neutralized MA-g-PP resin after the incubation period.

Filtrate solution at pH	Co^{2+} absorbance
3	0.480
4	0.495
5	0.480
6	0.456

Table A.3 Absorbance values for Cu^{2+} ion standard solutions in Cu^{2+} uptake testing of Ca^{2+} neutralized MA-g-PP resin.

Concentration (ppm)	Absorbance
2	0.066
5	0.161
10	0.299
20	0.553
30	0.795

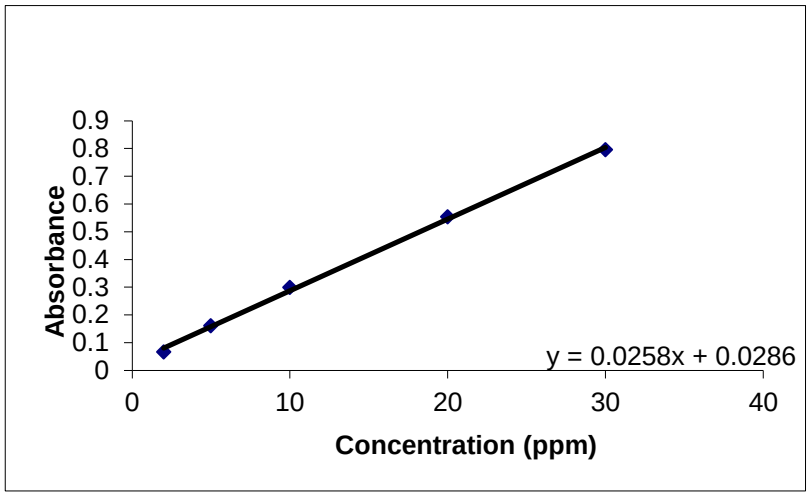

Figure A.2 Calibration curve for Cu^{2+} ion in Cu^{2+} uptake testing of Ca^{2+} neutralized MA-g-PP resin.

Table A.4 Absorbance values for Cu^{2+} of the filtrate solutions in Cu^{2+} uptake testing of Ca^{2+} neutralized MA-g-PP resin after the incubation period.

Filtrate solution at pH	**Cu^{2+} absorbance**
3	0.560
4	0.511
5	0.520
6	0.503

APPENDIX B

UPTAKE TEST RESULTS OF Na^+ NEUTRALIZED MA-g-PP RESIN

Table B.1 Absorbance values for Co^{2+} ion standard solutions in Co^{2+} uptake testing of Na^+ neutralized MA-g-PP resin.

Concentration (ppm)	Absorbance
2	0.073
5	0.179
10	0.347
20	0.554
30	0.703

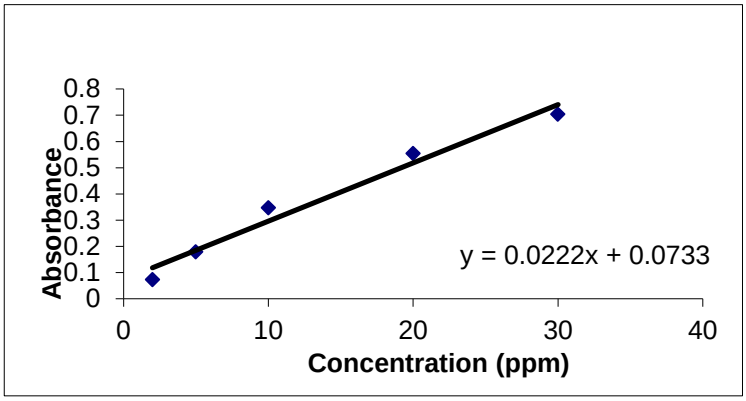

Figure B.1 Calibration curve for Co^{2+} ion in Co^{2+} uptake testing of Na^+ neutralized MA-g-PP resin.

Table B.2 Absorbance values for Co^{2+} of the filtrate solutions in Co^{2+} uptake testing of Na^{+} neutralized MA-g-PP resin after the incubation period.

Filtrate solution at pH	Co^{2+} absorbance
3	0.561
4	0.535
5	0.515
6	0.540

Table B.3 Absorbance values for Pb^{2+} ion standard solutions in Pb^{2+} uptake testing for Na neutralized MA-g-PP resin.

Concentration (ppm)	Absorbance
2	0.033
5	0.105
10	0.225
20	0.447
30	0.583

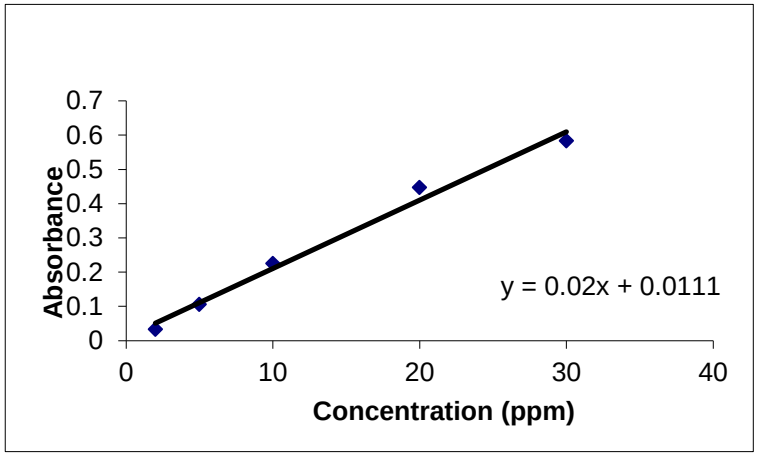

Figure B.2 Calibration curve for Pb^{2+} ion in Pb^{2+} uptake testing of Na^{+} neutralized MA-g-PP resin.

Table B.4 Absorbance values for Pb^{2+} of the filtrate solutions in Pb^{2+} uptake testing of Na^{+} neutralized MA-g-PP resin after the incubation period.

Filtrate solution at pH	Pb^{2+} absorbance
3	0.445
4	0.447
5	0.450
6	0.449

Table B.5 Absorbance values for Cu^{2+} ion standard solutions in Cu^{2+} uptake testing of Na^{+} neutralized MA-g-PP resin.

Concentration (ppm)	Absorbance
2	0.100
5	0.225
10	0.404
20	0.737
30	0.985

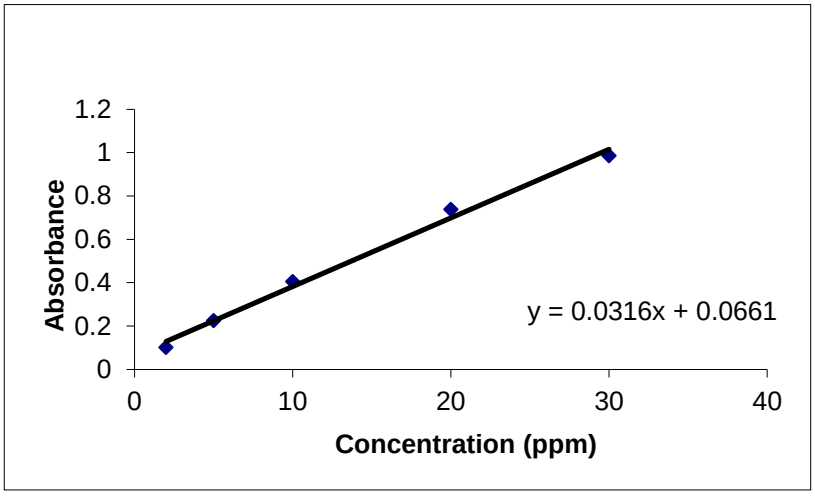

Figure B.3 Calibration curve for Cu^{2+} ion in Cu^{2+} uptake testing of Na^{+} neutralized MA-g-PP resin.

Table B.6 Absorbance values for Cu^{2+} of the filtrate solutions in Cu^{2+} uptake testing of Na^{+} neutralized MA-g-PP resin after the incubation period.

Filtrate solution at pH	Cu^{2+} absorbance
3	0.720
4	0.720
5	0.735
6	0.731

Table B.7 Absorbance values for Cd^{2+} ion standard solutions in Cd^{2+} uptake testing of Na^{+} neutralized MA-g-PP resin.

Concentration (ppm)	Absorbance
1	0.163
2	0.298
2.5	0.377
5	0.684
10	1.072
20	1.938

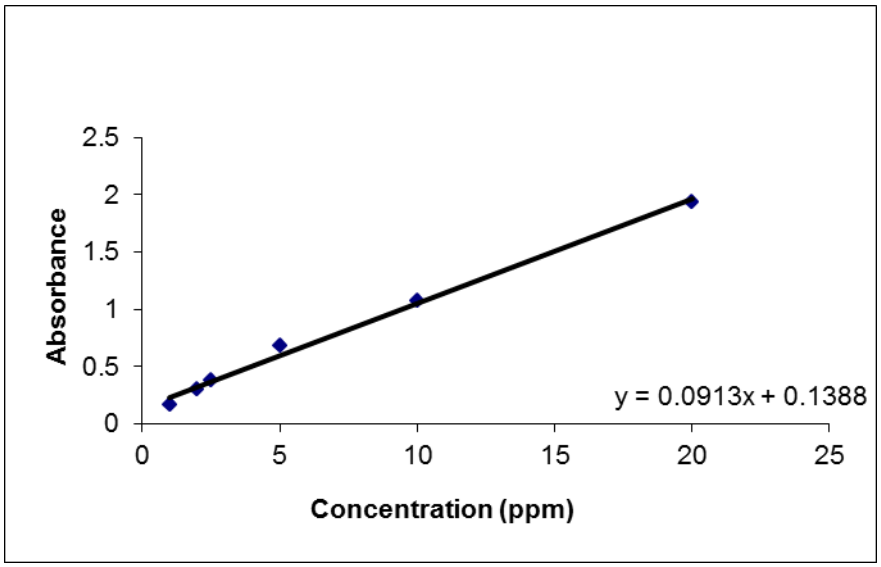

Figure B.4 Calibration curve for Cd^{2+} ion in Cd^{2+} uptake testing of Na^{+} neutralized MA-g-PP resin.

Table B.8 Absorbance values for Cd^{2+} of the filtrate solutions in Cd^{2+} uptake testing of Na^{+} neutralized MA-g-PP resin after the incubation period.

Filtrate solution at pH	**Cd^{2+} absorbance**
3	1.946
4	1.940
5	1.938
6	1.941

APPENDIX C

UPTAKE TEST RESULTS OF OF Mg^{2+} NEUTRALIZED MA-g-PP RESIN

Table C.1 Absorbance values for Co^{2+} ion standard solutions in Co^{2+} uptake testing of Mg^{2+} neutralized MA-g-PP resin.

Concentration (ppm)	Absorbance
2	0.073
5	0.179
10	0.347
20	0.554
30	0.703

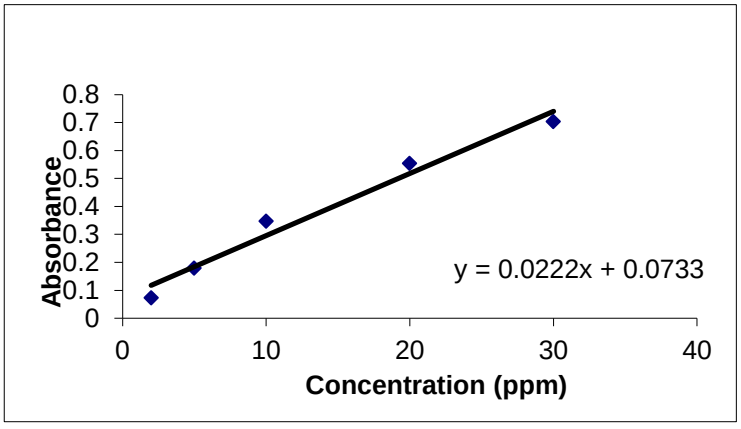

Figure C.1 Calibration curve for Co^{2+} ion in Co^{2+} uptake testing of Mg^{2+} neutralized MA-g-PP resin.

Table C.2 Absorbance values for Co^{2+} of the filtrate solutions in Co^{2+} uptake testing of Mg^{2+} neutralized MA-g-PP resin after the incubation period.

Filtrate solution at pH	Co^{2+} absorbance
3	0.555
4	0.550
5	0.550
6	0.561

Table C.3 Absorbance values for Pb^{2+} ion standard solutions in Pb^{2+} uptake testing of Mg^{2+} neutralized MA-g-PP resin.

Concentration (ppm)	Absorbance
2	0.032
5	0.093
10	0.202
20	0.381
30	0.518

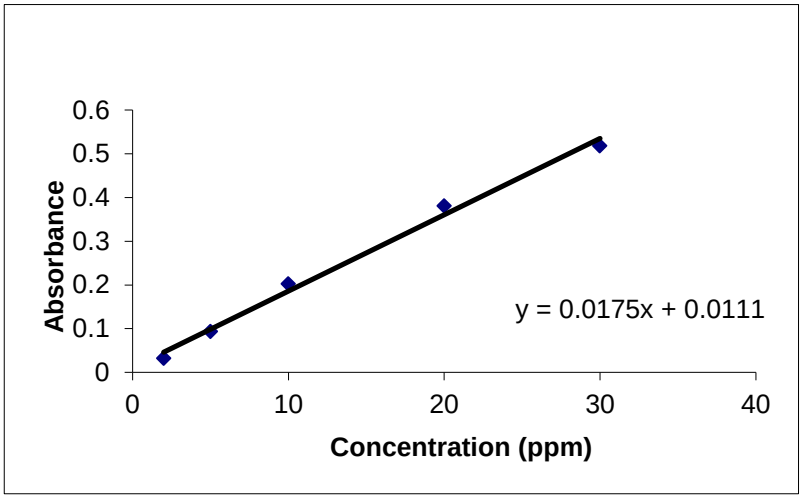

Figure C.2 Calibration curve for Pb^{2+} ion in Pb^{2+} uptake testing of Mg^{2+} neutralized MA-g-PP resin.

Table C.4 Absorbance values for Pb^{2+} of the filtrate solutions in Pb^{2+} uptake testing of Mg^{2+} neutralized MA-g-PP resin after the incubation period.

Filtrate solution at pH	Pb^{2+} absorbance
3	0.380
4	0.395
5	0.380
6	0.366

Table C.5 Absorbance values for Cu^{2+} ion standard solutions in Cu^{2+} uptake testing of Mg^{2+} neutralized MA-g-PP resin.

Concentration (ppm)	Absorbance
2	0.100
5	0.225
10	0.404
20	0.737
30	0.985

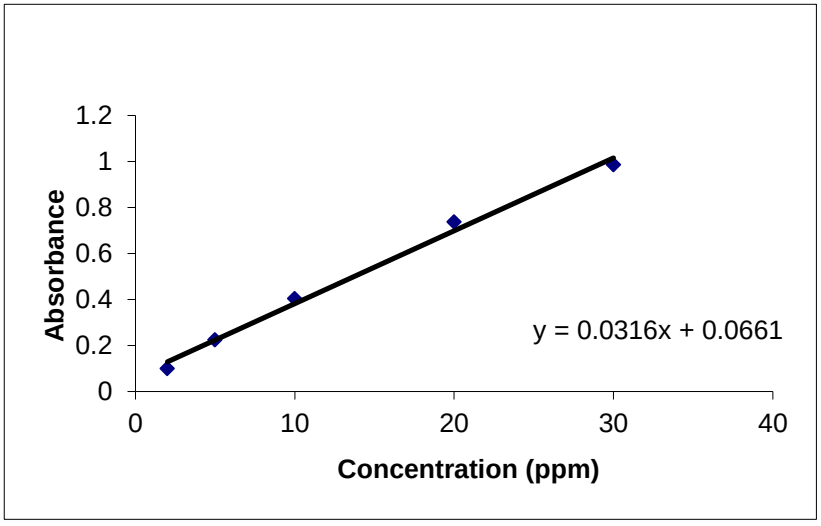

Figure C.3 Calibration curve for Cu^{2+} ion in Cu^{2+} uptake testing of Mg^{2+} neutralized MA-g-PP resin.

Table C.6 Absorbance values for Cu^{2+} of the filtrate solutions in Cu^{2+} uptake testing of Mg^{2+} neutralized MA-g-PP resin after the incubation period.

Filtrate solution at pH	Cu^{2+} absorbance
3	0.735
4	0.736
5	0.740
6	0.723

Table C.7 Absorbance values for Cd^{2+} ion standard solutions in Cd^{2+} uptake testing of Mg^{2+} neutralized MA-g-PP resin.

Concentration (ppm)	Absorbance
1	0.163
2	0.298
2.5	0.377
5	0.684
10	1.072
20	1.938

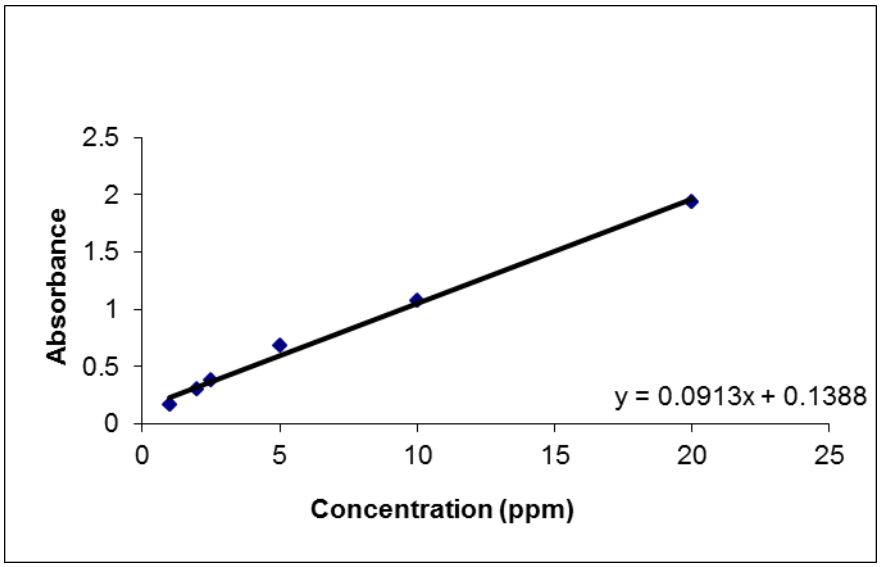

Figure C.4 Calibration curve for Cd^{2+} ion in Cd^{2+} uptake testing of Mg^{2+} neutralized MA-g-PP resin.

Table C.8 Absorbance values for Cd^{2+} of the filtrate solutions in Cd^{2+} uptake testing of Mg^{2+} neutralized MA-g-PP resin after the incubation period.

Filtrate solution at pH	**Cd^{2+} absorbance**
3	1.942
4	1.939
5	1.940
6	1.940

APPENDIX D

UPTAKE TEST RESULTS OF K^+ NEUTRALIZED MA-G-PP RESIN

Table D.1 Absorbance values for Co^{2+} ion standard solutions in Co^{2+} uptake testing of K^+ neutralized MA-g-PP resin.

Concentration (ppm)	Absorbance
2	0.004
5	0.012
10	0.027
20	0.056
30	0.091

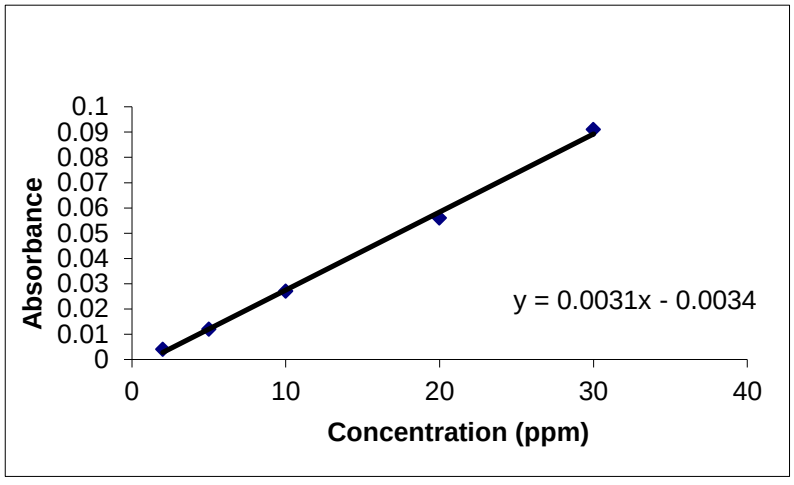

Figure D.1 Calibration curve for Co^{2+} ion in Co^{2+} uptake testing of K^+ neutralized MA-g-PP resin.

Table D.2 Absorbance values for Co^{2+} of the filtrate solutions in Co^{2+} uptake testing of K^{+} neutralized MA-g-PP resin after the incubation period.

Filtrate solution at pH	Co^{2+} absorbance
3	0.063
4	0.061
5	0.060
6	0.063

Table D.3 Absorbance values for Pb^{2+} ion standard solutions in Pb^{2+} uptake testing of K^{+} neutralized MA-g-PP resin.

Concentration (ppm)	Absorbance
5	0.011
10	0.025
20	0.045
30	0.074
40	0.105
60	0.149
70	0.183

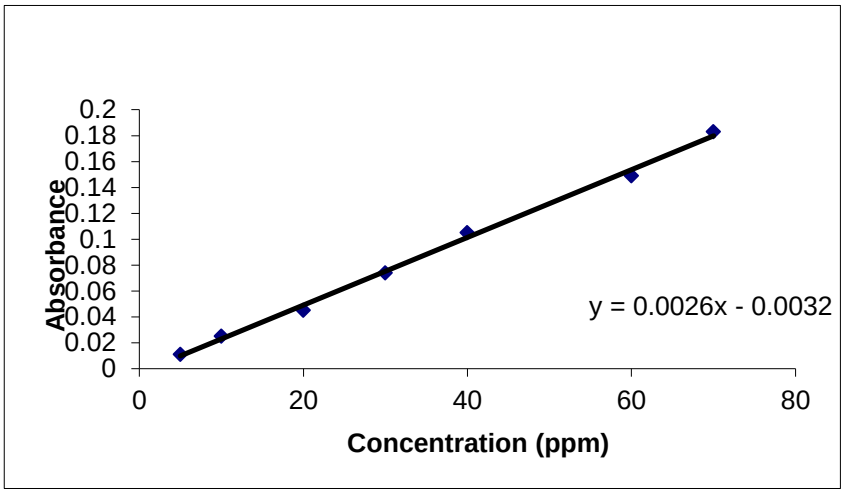

Figure D.2 Calibration curve for Pb^{2+} ion in Pb^{2+} uptake testing of K^{+} neutralized MA-g-PP resin.

Table D.4 Absorbance values for Pb^{2+} of the filtrate solutions in Pb^{2+} uptake testing of K^{+} neutralized MA-g-PP resin after the incubation period.

Filtrate solution at pH	Pb^{2+} absorbance
3	0.045
4	0.043
5	0.040
6	0.045

Table D.5 Absorbance values for Cu^{2+} ion standard solutions in Cu^{2+} uptake testing of K^{+} neutralized MA-g-PP resin.

Concentration (ppm)	Absorbance
2	0.024
5	0.055
10	0.103
20	0.219
30	0.291

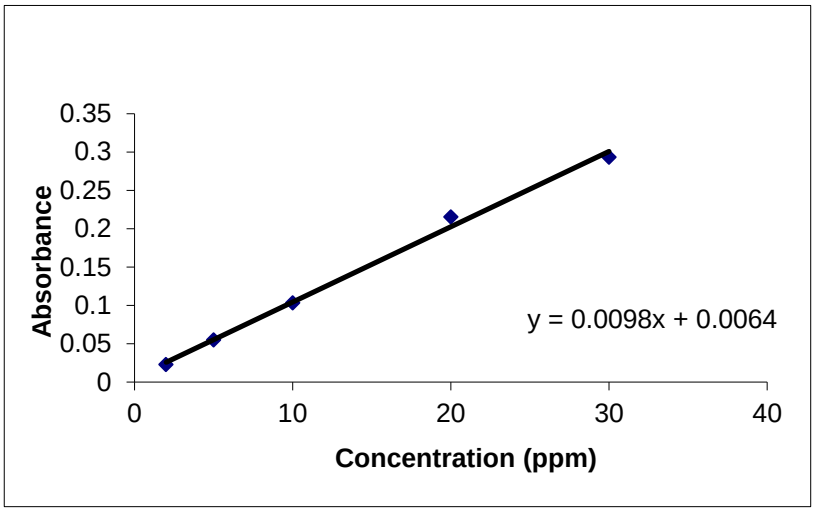

Figure D.3 Calibration curve for Cu^{2+} ion in Cu^{2+} uptake testing of K^{+} neutralized MA-g-PP resin.

Table D.6 Absorbance values for Cu^{2+} of the filtrate solutions in Cu^{2+} uptake testing of K^{+} neutralized MA-g-PP resin after the incubation period.

Filtrate solution at pH	Cu^{2+} absorbance
3	0.203
4	0.208
5	0.206
6	0.206

Table D.7 Absorbance values for Cd^{2+} ion standard solutions in Cd^{2+} uptake testing of K^{+} neutralized MA-g-PP resin.

Concentration (ppm)	Absorbance
2	0.049
5	0.140
10	0.296
20	0.630
30	0.879

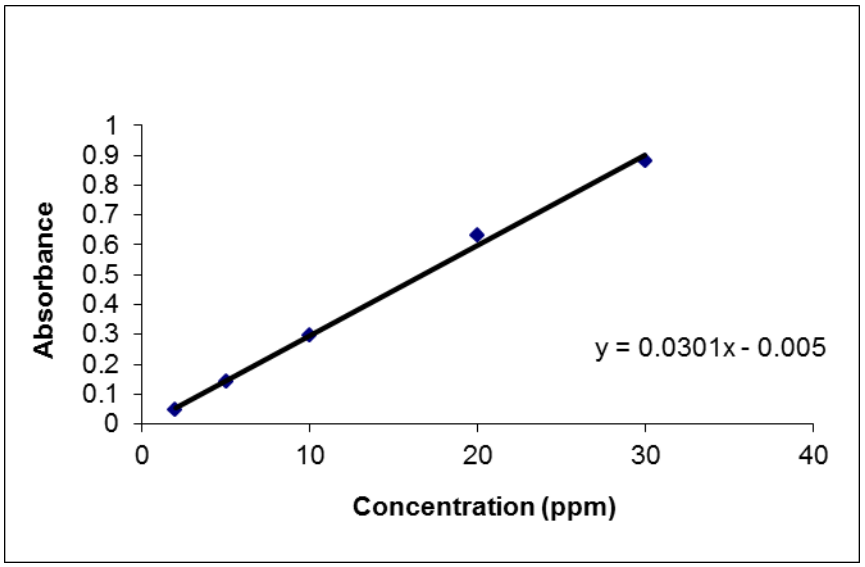

Figure D.4 Calibration curve for Cd^{2+} ion in Cd^{2+} uptake testing of K^{+} neutralized MA-g-PP resin.

Table D.8 Absorbance values for Cd^{2+} of the filtrate solutions in Cd^{2+} uptake testing of K^{+} neutralized MA-g-PP resin after the incubation period.

Filtrate solution at pH	**Cd^{2+} absorbance**
3	0.627
4	0.625
5	0.628
6	0.625

APPENDIX E

UPTAKE TEST RESULTS OF NON-NEUTRALIZED MA-g-PP RESIN

Table E.1 Absorbance values for Co^{2+} ion standard solutions in Co^{2+} uptake testing of non-neutralized MA-g-PP resin.

Concentration (ppm)	Absorbance
2	0.004
5	0.010
10	0.024
20	0.061
30	0.091

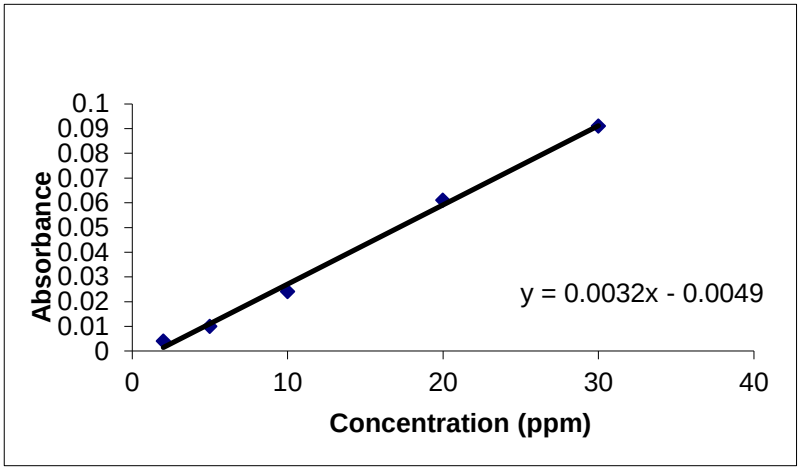

Figure E.1 Calibration curve for Co^{2+} ion in Co^{2+} uptake testing of non-neutralized MA-g-PP resin.

Table E.2 Absorbance values for Co^{2+} of the filtrate solutions in Co^{2+} uptake testing of non-neutralized MA-g-PP resin after the incubation period.

Filtrate solution at pH	Co^{2+} absorbance
3	0.060
4	0.064
5	0.064
6	0.062

Table E.3 Absorbance values for Pb^{2+} ion standard solutions in Pb^{2+} uptake testing of non-neutralized MA-g-PP resin.

Concentration (ppm)	Absorbance
5	0.011
10	0.025
20	0.045
30	0.074
40	0.105
60	0.149
70	0.183

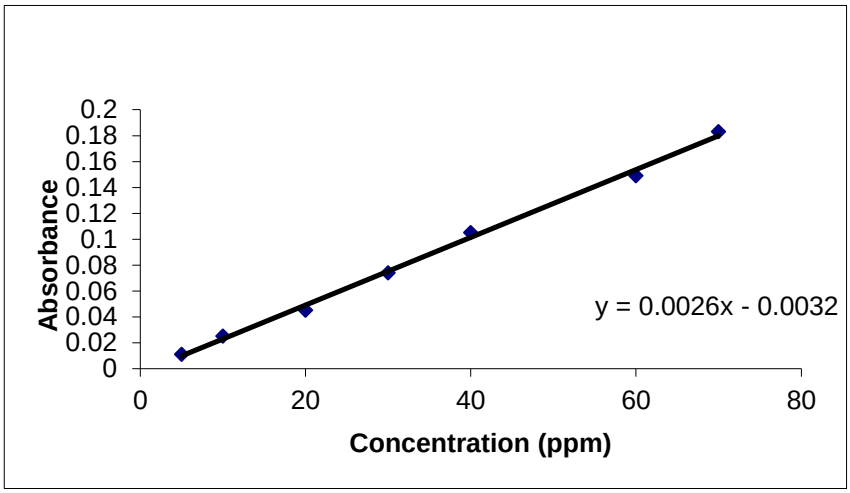

Figure E.2 Calibration curve for Pb^{2+} ion in Pb^{2+} uptake testing of non-neutralized MA-g-PP resin.

Table E.4 Absorbance values for Pb^{2+} of the filtrate solutions in Pb^{2+} uptake testing of non-neutralized MA-g-PP resin after the incubation period.

Filtrate solution at pH	Pb^{2+} absorbance
3	0.050
4	0.048
5	0.051
6	0.052

Table E.5 Absorbance values for Cu^{2+} ion standard solutions in Cu^{2+} uptake testing of non-neutralized MA-g-PP resin.

Concentration (ppm)	Absorbance
2	0.023
5	0.055
10	0.103
20	0.215
30	0.293

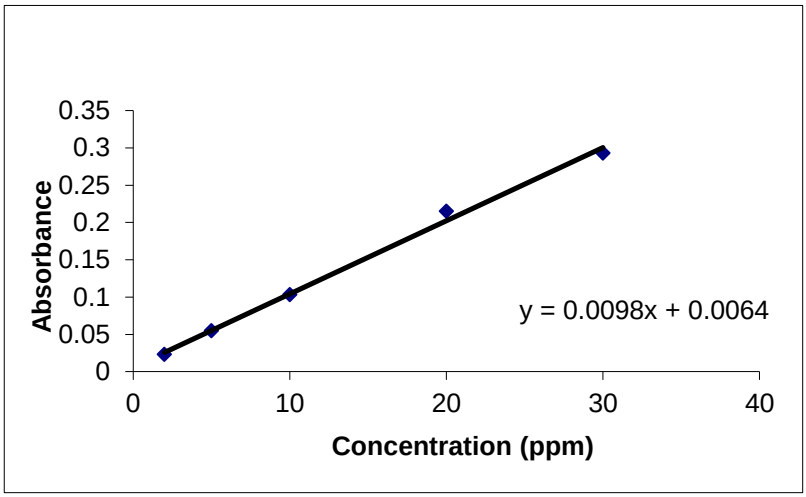

Figure E.3 Calibration curve for Cu^{2+} ion in Cu^{2+} uptake testing of non-neutralized MA-g-PP resin.

Table E.6 Absorbance values for Cu^{2+} of the filtrate solutions in Cu^{2+} uptake testing of non-neutralized MA-g-PP resin after the incubation period.

Filtrate solution at pH	Cu^{2+} absorbance
3	0.210
4	0.206
5	0.205
6	0.206

Table E.7 Absorbance values for Cd^{2+} ion standard solutions in Cd^{2+} uptake testing of non-neutralized MA-g-PP resin.

Concentration (ppm)	Absorbance
2	0.049
5	0.140
10	0.296
20	0.630
30	0.879

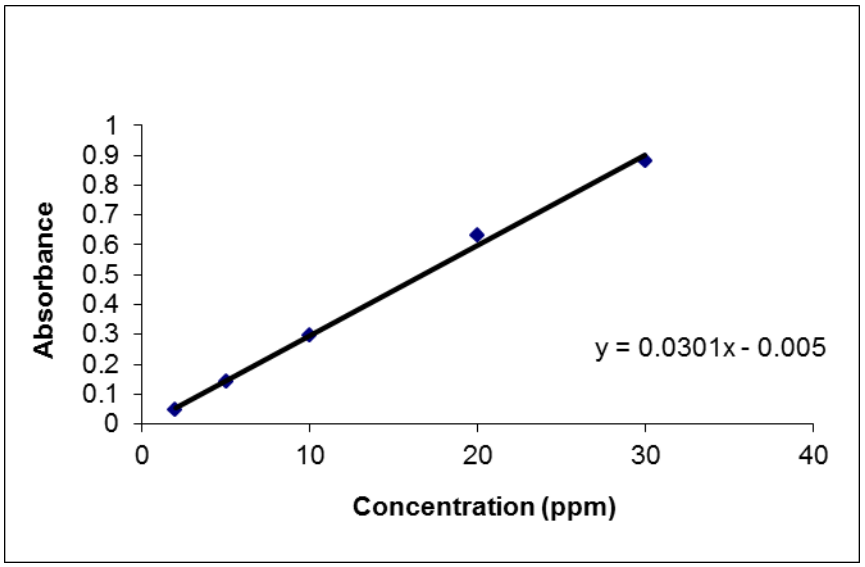

Figure E.4 Calibration curve for Cd^{2+} ion in Cd^{2+} uptake testing of non-neutralized MA-g-PP resin.

Table E.8 Absorbance values for Cd^{2+} of the filtrate solutions in Cd^{2+} uptake testing of non- neutralized MA-g-PP resin after the incubation period.

Filtrate solution at pH	**Cd^{2+} absorbance**
3	0.611
4	0.621
5	0.626
6	0.623

CURRICULUM VITAE

PERSONAL INFORMATION

Surname, Name: Ecevit Safiye Tuba
Nationality: Turkish (TC)
Date and Place of Birth: 10 July 1978 , Ankara
Marital Status: Single
Phone: +90 312 295 88 03
Fax: +90 312 210 32 00
email: stecevit@yahoo.com

EDUCATION

Degree	Institution	Year of Graduation
MS METU	Polymer Science and Technology	2004
BS METU	Chemistry	2001
High School	Kocatepe Mimar Kemal High School	

WORK EXPERIENCE

Year	Place	Enrollment
2006-Present	Turkis Atomic Energy Authority	Chemist
2001-2006	Ministry of Natioanal Education	English Teacher

FOREIGN LANGUAGES

Advanced English

PUBLICATIONS

1. S.T. Ecevit, L. Aras and T. Tinçer, Synthesis and Characterization of Surface Sulfonated Polypropylene" Vol.22, 1285-1299 2008. *"J. Adhesion Sci. and Technology"*, 22, (2008), p.1285-1299

HOBBIES

Movies, Swimming, Running.